STACKING SEQUENCE OPTIMIZATION AND MODELING OF LAMINATED COMPOSITE PLATES FOR FREE VIBRATION

A Thesis Submitted to
the Graduate School of Engineering and Sciences of
İzmir Institute of Technology
in Partial Fulfillment of the Requirements for the Degree of

MASTER OF SCIENCE

in Mechanical Engineering

by
Emre Azim HASANOĞLU

January 2018
İZMİR

We approve the thesis of **Emre Azim HASANOĞLU**

Examining Committee Members:

_____

Assoc. Prof. Dr. H. Seçil ARTEM
Department of Mechanical Engineering, İzmir Institute of Technology

_____

Assist. Prof. Dr. Kasım TOPRAK
Department of Mechanical Engineering, İzmir Institute of Technology

_____

Assist. Prof. Dr. Ebubekir ATAN
Department of Mechanical Engineering, İzmir Katip Çelebi University

04 January 2018

_____

Assoc. Prof. Dr. H. Seçil ARTEM
Supervisor, Department of Mechanical Engineering, İzmir Institute of Technology

_____

Prof. Dr. Metin TANOĞLU
Head of the Department of Mechanical Engineering

_____

Prof. Dr. Aysun SOFUOĞLU
Dean of the Graduate School of Engineering and Sciences

ACKNOWLEDGMENTS

I would like to thank and express my deep sense of gratitude and indebtedness to my advisor Assoc. Prof. Dr. H. Seçil ARTEM for her invaluable advice, immense knowledge, continuous support and encouragement. Her guidance helped me in all the time of research and writing of this thesis. I could not have imagined having a better advisor and mentor for my thesis.

Besides my advisor, I would also like to show my sincere thanks to Assist. Prof. Dr. Levent AYDIN and Res. Assist. H. Arda DEVECİ for his guidance, support and encouragement, which made my dissertation a better work.

Finally, special thanks to my family for their endless understanding, supports, motivation, continuous advice and love in all my life and believing in me. I am always sure that they are happy to be there for me. I cannot even imagine how much they contribute efforts for me.

ABSTRACT

STACKING SEQUENCE OPTIMIZATION AND MODELING OF LAMINATED COMPOSITE PLATES FOR FREE VIBRATION

Composite materials, especially fiber reinforced composites, have been extensively used in various engineering fields such as automotive, aerospace, aircrafts, defense, marine and so on due to having their high specific strength to weight and stiffness to weight ratios. In these last years, vibration problem has become more and more important in the structures where thin plates are used. Therefore, free vibration characteristics of composite structures under the influence of dynamic forces should be determined in the design process. Accordingly, in this thesis, optimum designs, which maximize the natural frequencies of laminated composite plate, are investigated by using hybrid algorithm combining the genetic algorithm (GA) and generalized pattern search algorihm (GPSA). Composite plates made of graphite/epoxy have been considered and assumed to be symmetric with continuous fiber angles in the laminate sequences. The natural frequency of plates is obtained bu using the Rayleigh Ritz method analytically. Free vibration equation is taken as objective function and fiber orientation angles are chosen as design variables. The natural frequency is maximized for various boundary conditions, aspect ratios, number of ply and material properties. The optimum designs obtained are verified by finite element method, and mode shapes of laminated composite plates are presented. A comparison between continuous and conventional (laminate in which the orientation angles are limited to the conventional orientations) designs is performed in order to show the reliability of continuous plates. As a results, it is observed that material properties, boundary conditions and dimensions of composite plates play important role on vibration behavior of composite plates. On the other hand, the natural frequencies and the optimum fiber oriantation angles are not affected from the change of number of plies.

ÖZET

SERBEST TİTREŞİM İÇİN TABAKALI KOMPOZİT PLAKALARIN TABAKA DİZİLİMLERİNİN OPTİMİZASYONU VE MODELLENMESİ

Kompozit malzemeler, özellikle fiber takviyeli kompozitler, düşük ağırlıklarına karşın yüksek mukavemet ve dayanıma sahip olmalarından dolayı, otomobil, havacılık, savunma ve denizcilik gibi birçok mühendislik uygulamalarında yoğun bir şekilde kullanılmaktadır. Son yıllarda, ince plakların ağırlıklı olarak kullanıldığı yapılarda titreşim problemi giderek daha da önemli hale geldi. Bu nedenle dinamik kuvvet etkisi altında olan kompozit yapıların serbest titreşim karekteristikleri daha tasarım aşamasındayken belirlenmelidir. Dolayısıyla, bu tezde, tabakalı kompozit plakaların ilk doğal frekansını maksimize eden optimum tasarımlar genetik algoritma (GA) ve genelleştirilmiş model arama algoritmasının (GPSA) kombinasyonu ile oluşan hibrit algoritma kullanılarak araştırılmıştır. Grafit/epoksi malzemesinden yapılmış olan plakların levha dizilimleri sürekli fiber açılara sahip olacak şekilde simetrik olarak seçilmiştir. Plakaların doğal frekansı Rayleigh Ritz metodu kullanılarak analitik olarak elde edilmiştir. Serbest titreşim denklemi amaç fonksiyonu ve fiber oryantasyonları tasarım değişkeni olarak alınmıştır. Plakaların doğal frekansı çeşitli sınır şartları, plaka en-boy oranı, tabaka sayısı ve malzeme özellikleri için maksimize edilmiştir. Elde edilen optimum tasarımlar sonlu elemanlar analizi yöntemiyle doğrulanmış ve kompozit plakaların titreşim sonucunda oluşan mode şekilleri belirlenmiştir. Sürekli ve belirli plaka (açıları geleneksel dizilimlerle sınırlanmış levha) tasarımları arasında bir kıyaslama yapılarak, sürekli tasarımların güvenilirliğini gösterilmiştir. Sonuç olarak, malzeme özellikleri, sınır şartları ve plaka ölçülerinin tabakalı kompozit plakaların titreşim davraşını kritik öneme sahip olduğu gözlemlenmiştir. Tabaka sayısındaki değişimin ise, plakaların optimum fiber oryantasyon açılarını ve doğal frekanları etkilemediği tespit edilmiştir.

TABLE OF CONTENTS

LIST OF FIGURES viii

LIST OF TABLES x

CHAPTER 1. INTRODUCTION 1
1.1.Literature Survey 1

CHAPTER 2. COMPOSITE MATERIALS 6
2.1. Introduction 6
2.2. Types and Classification of Composite Materials 10
2.3. Application of Composite Materials 14

CHAPTER 3. MECHANICS OF COMPOSITE MATERIALS 17
3.1. Introduction 17
3.2. Classical Lamination Theory 18
3.3. Vibration Analysis of Laminated Composite Plate 23
3.3.1. All Sides Simply Supported 24
3.3.2. Different Boundary Conditions 30

CHAPTER 4. OPTIMIZATION 35
4.1. General Information 35
4.2. Definition of Optimization Problem 37
4.3. Genetic Algorithm (GA) 38
4.3.1. Crossover 39
4.3.2. Mutation 39
4.3.3. Selection 40
4.4. Generalized Pattern Search Algorithm (GPSA) 40
4.5. Matlab Optimization Toolbox 42
4.5.1. Hybrid Algorithm Solver 44

CHAPTER 5. FINITE ELEMENT METHOD 46
5.1. Introduction 46
5.2. General Steps of Finite Element Method 47
5.3. Finite Element Modeling Using ANSYS 49
5.4. Modal Analysis in ANSYS 51

CHAPTER 6. RESULTS AND DISCUSSIONS 54
6.1. Problem Definition 54
6.2. The Verification of Algorithms and Modeling 56
6.3. Optimization Results and Discussion 63

CHAPTER 7. CONCLUSIONS 79

REFERENCES 81

APPENDICES
APPENDIX A. MATLAB COMPUTER PROGRAM 84
APPENDIX B. ANSYS APDL CODE 86

LIST OF FIGURES

Figure **Page**

Figure 2.1. Relative importance of material development through history 7
Figure 2.2. Lamina and laminate lay-ups 9
Figure 2.3. Classification of composite materials 12
Figure 2.4. Composite components used in military aircraft..... 14
Figure 2.5. Composite components used in satellite components 15
Figure 2.6. First fiberglass corvette body parts 16
Figure 3.1. Levels of observation and types of analysis for composite materials 18
Figure 3.2. A thin fiber-reinforced laminated composite subjected to in plane loading.....19
Figure 3.3. Coordinate locations of plies in a laminate 19
Figure 3.4. Coordinate system for rectangular plate..... 31
Figure 4.1. Minimum and maximum of objective function ($f(x)$) 36
Figure 4.2. Types of crossover (a) One-point crossover (b) Two-point crossover..... 39
Figure 4.3. Value-altering mutation of strings (a) Single-gene mutation (b) Multi-gene mutation (c) Multi-gene mutation 40
Figure 4.4. Matlab optimization toolbox ga solver user interface 42
Figure 4.5. Flowchart of the hybrid algorithm optimization 45
Figure 5.1. Typical finite element mesh 47
Figure 5.2. Simple one-dimensional line element 48
Figure 5.3. Simple two-dimensional elements with corner nodes and intermediate nodes..... 48
Figure 5.4. Simple three-dimensional elements with corner nodes and intermediate nodes..... 48
Figure 5.5. 8 node 281 shell element..... 50
Figure 5.6. Mode shapes of the cantilever beam model 51
Figure 5.7. Modal analysis options in ANSYS..... 53
Figure 6.1. Edge numbering and coordinate system of the laminated composite plate . 54
Figure 6.2. The finite element model of symmetric 8-layered composite plate 57
Figure 6.3. Mesh convergence for all aspect ratios 58
Figure 6.4. The mode shapes and fundamental frequencies Ω_{opt} for a/b=1 61

Figure 6.5. The mode shapes and fundamental frequencies Ω_{opt} for *a/b*=2 62
Figure 6.6. Comparison of the optimum frequency Ωopt of symmetric 8-layered composite plate between conventional and continuous designs for different aspect ratios..... 76
Figure 6.7. Comparison of the hybrid algorithm and GA results for symmetrical laminated rectangular plates having CSCF and SSSF edge conditions (a/b=4) 77
Figure 6.8. The best and mean values of the objective functions at each generation in GA for (a) a/b=1, (b) a/b=2, (c) a/b=3, (d) a/b=4, (e) a/b=5..... 78

LIST OF TABLES

Table **Page**

Table 2.1. Tensile properties of some metallic and structural composite..... 8

Table 2.2. Types of laminated composite materials 11

Table 3.1. The elements of the matrix [G]..... 29

Table 3.2. Displacement function of a freely vibrating plates..... 32

Table 3.3. Coefficients for orthotropic rectangular plate..... 33

Table 4.1. Genetic Algorithm parameters for single objective function 43

Table 6.1. The elastic properties of graphite/epoxy layers 55

Table 6.2. Verification of objective function algorithm and finite element modeling for symmetric 8-layered square plate with various boundary conditions (a/b = 1) 59

Table 6.3. Verification of objective function algorithm and finite element modeling for symmetric 8-layered plate with various boundary conditions (a/b = 2) 60

Table 6.4. Optimum stacking sequence for symmetric 4-layered composite plate 63

Table 6.5. Optimum stacking sequence for symmetric 8-layered composite plate 66

Table 6.6. Optimum stacking sequence for symmetric 16-layered composite plate 69

Table 6.7. Effect of degree of orthotropy for symmetric 8-layered composite plate 73

Table 6.8. The comparison between conventional and continuous designs for symmetrical 8-layered composite plate..... 74

CHAPTER 1

INTRODUCTION

1.1. Literature Survey

Composite materials, especially fiber reinforced composites, have been extensively used in various engineering fields such as automotive, aerospace, aircrafts, defense, marine and so on. They have unprecedented mechanical and physical properties because composites are multifunctional material combining the best properties of different materials. Rapid technological developments and increasing competition in the industry necessitate the design of product having low weight, high strength or stiffness and better mechanical properties than the other materials. Composite materials have become the best choice which satisfies these requirements in structural application today and for the future. The anisotropic nature of fiber - reinforced composites provides opportunities for tailoring appropriate fiber materials and ply orientations. Although the high strength-to-weight properties of composite materials are attractive, due to the reasons like a high cost and production difficulty, all parameters should be optimized by the designer according to the specific requirements in design stage. Fiber orientations, layer thickness, stacking sequences, geometric parameters, cost and weight are taken to be design variables to improve the performance of components.

Many researchers have carried out the studies comprehensively on vibration of laminated composite plates by making use of different optimization techniques to achieve optimum structure. In the literature, different classifications are available for optimization of composite laminates. For example, Fang and Springer (1993) identified four categories for the optimization methods, namely: (1) analytical procedures, (2) enumeration methods (trial of all configurations), (3) stochastic search methods, and (4) non-linear programming. The correct selection of an optimization method is of great importance for solution of the problem. The aproppriate optimization method may be chosen depending on the type of problem and type of functions such as convex, nonconvex, continuous and discontinuous.

Many structural components are generally subjected to dynamic forces during their functional life. As well as the excitation frequency, all structures have natural frequency at which the system naturally tends to vibrate. Thus, resonance occurs when the excitation frequency coincides with the natural frequencies of system. To avoid fracture of materials due to the vibration, natural frequency, especially fundamental one, becomes important design criteria along with the increase of velocity and the decrease of weight in the structures. Fundamental frequency gets lower with the decreased thickness. If the structure are not subjected to high forcing frequency, the risk of resonance may be decreased by maximizing fundamental frequency. Accordingly, some researchers have tried to maximize fundamental frequency of laminate. One of the first studies on optimal design of composites was done by Bert (1977), who considered the fiber orientation angle of each layer as a continuous design variable for single-objective fundamental frequency maximization of a simply supported symmetric balanced laminate. Bert (1978) also proposed the same study in clamped edge conditions. In both of these studies, closed-form solution was performed for natural frequency which takes account of the effects of bend-twist coupling in an approximate. An analytical closed form optimal solution for thin rectangular laminated plates based on the classical lamination theory has been carried out by Reiss and Ramachandran (1987). Grenestedt (1989) calculated the lowest free vibration frequency both numeric by means of finite element method and analytic with perturbation approach. Mateus et al. (1991) have made sensitivity analysis and optimal design study for thin laminated composite materials by using finite element method and obtained results for maximum fundamental frequency and minimum elastic strain energy. Ply thicknesses and orientation angles in all of these studies were taken as continuous variable for design optimization of composite materials. If the structure subjects to high forcing frequency, it is desirable that external forcing frequency stays between two adjacent higher order natural frequencies. In this case, maximizing the gap between these frequencies reduce the likelihood of resonance. Some of researchers have investigated the problem of maximum frequency separation. Optimal fiber orientation of antisymmetric hybrid laminates for maximum fundamental frequency and frequency separation are studied by Duffy and Adali (1991). Adali and Verijenko (2001) determined the optimum stacking sequences of symmetric hybrid laminates consisting of high-stiffness surface and low-stiffness core layer undergoing free vibrations. The fiber orientations are limited with

four different angles, which directly reduce the computational time. Also, the effect of hybridization is evaluated for the aspect ratio and the number of plies in both of studies.

In many of the previous studies, analytical and enumeration methods are used as optimization method to find frequency response of structure. Analytical method is gradient-based search techniques. It requires to the gradient information of the objective function and/or constraints to express the decreasing direction of the objective function, which isn't mostly available in many complex problems. They are also sensitive to starting point and probably converge to worse local minumum near starting point instead of the global optimum in a complex design space, which means it may be 'trapped' to local minima. Consequently, most of the analytical optimization methods are insufficient in determining minimum value of multivariate function. Enumeration method is the simplest of optimization techniques. The principle of this method is based on evaluating all combinations of the discrete variables. Use of enumeration method ensures obtaining the best configuration for the structure, but it takes a very long time to solve especially problems having large design spaces.

As opposed to these optimization methods, stochastic methods are being used to overcome these disadvantages. Researchers often resort to these methods to successfully solve optimization problems having complex design space. These methods can obtain the globally optimal configuration without being sensitive to the starting point and they do not need the differentiation of objective function. Various stochastic algorithms, such as genetic algorithm (GA), ant colony optimization (ACO), simulated annealing (SA) and tabu search (TS) are commonly used in composite optimization.

Abachizadeh and Tahani (2008) investigated optimal design of symmetrical hybrid laminates and minimum cost by using ant colony optimization algorithm. Hybrid structure is composed of high stiffness materials on surface layer and low stiffness material in core layers. They demonstrated effectiveness of the hybridization concept on reducing weight. Karakaya and Soykasap (2011) have found optimal fiber oriantation to maximize natural frequency and buckling loads of simply supported hybrid composite plates by using genetic algorithm and simulated annealing and was also compared effectiveness of two different optimization techniques. The best fiber oriantation is identified for different aspect ratio. Natural frequency response for symmetrically laminated composite plate was optimized by Kayıkcı and Sonmez (2012), who considered two different problem; frequency separation maximization and fundamental frequency maximization. Due to the existence of numerious local optimums, direct

simulated annealing was utilized to find the optimal configuration in various aspect ratios. Hemmatian et al. (2013) studied minimum cost and minimum weight optimizing the number and angle of layer by using elitist ant system optimization methods. Material, thickness and number of surface and core layer were taken as the desing variables in the optimization process. Topal et al. (2017) presented a study based on teaching-learning optimization for fundamental frequency of simply supported antisymetric laminated composite plate. First order shear deformation theory taking into account traverse shear strain was used as analytic formulation.

Natural frequencies of composite plates can be calculated via either analytical or approximate solution methods. It is naturally desirable to obtain the analytical solution, but not always easily attainable as in case of the plates with mixed boundary conditions or plates with irregular boundaries. Since the analytic expressions for a rectangular plate can be solved by using Navier solution technique when all four edges of the laminate are simply supported, most of the researchers have focused on vibration analysis of laminated plates under simply supported boundary condition. On the other hand, edge constraints significantly affects the natural frequency of flat plates and also, plate structure may be found in different edge constraints under its working conditions. For these reasons, approximate solution methods like the Rayleigh Ritz method, Galerkin method and finite element method have been developed. One of first studies having complex boundary conditions has been done by Fan and Cheung (1984). They have analyzed the rectangular plate by the help of finite strip method. Qatu (1991) used higher-order mixed theory to find natural frequency of plate in various boundary conditions, material parameters and fiber orientations. Narita (2003) introduced a Ritz-based layerwise optimization approach for symmetric composite plates. His approach finds the fiber oriantation angles from outer layer to inner layer, respectively and obviously reduces the computation time. Apalak et al. (2008) determined the optimal layer sequences of the symmetrical composite plates using genetic algorithm, artificial neural networks and finite element method. Sadr and Bargh (2012) studied on fundamental frequency optimization of symmetrically laminated composite plates by using elitist-genetic algorithm. Fitness function is computed semi-analytical finite strip approach based on classical lamination theory, which is developed on the basis of energy methods. Fiber oriantation angles, edge conditions and plate lenght/width ratios are considered as the design variables.

In this thesis, optimal stacking sequence designs of symetrically laminated composite plates made of graphite/epoxy for maximum vibration resistance are determined by using hybrid algorithm combining genetic algorihm (GA) in global search procedure and generalized pattern search algorihm (GPSA) in a local search procedure. Composite plates in optimum fiber oriantation angles are then modeled by using the finite element method (FEM) to verify the natural frequency values and optimum fiber oriantation angles obtained at the result of optimization. Effect of different parameters such as the number of layers, boundary conditions, plate lenght/width ratios and material properties on the vibration behavior of laminated composite plate is discussed.

CHAPTER 2

COMPOSITE MATERIALS

2.1. Introduction

In general sense, a composite is commonly defined as a structural material that is made from two or more constituents which are combined at a macroscopic level and are not soluble in each other. One constituent is called the reinforcing phase and the other one in which it is embedded is named as the matrix. The reinforcing phase may be in the different form like fibers, particles, and flakes, and materials of the reinforcing phase are ceramics, metal, polymers or elements such as carbon and boron. The matrix phase materials are generally continuous (Kaw, 2006). The above explanation including metals alloys, plastic co-polymers, minerals, and wood is more general. Fiber-reinforced composite materials which are most common form of composite material differ from the above materials because the constituent materials are different at the molecular level and are mechanically separable. Fiber-reinforced composite materials are composed of fibers and matrix. Fiber and matrix generate a new material by remaining in their original form. Composite materials obtained have significantly different physical or chemical properties than constituent material properties (Mazumdar, 2002).

The history of fiber-reinforcement is quite old. For instance, the ancient egyptians used chopped straw in bricks to be stronger. Wood is example of natural composites and available for tens thousands of year. Furthermore; mud huts were constructed from mixture of grasses and thin sticks by Africans. In the 20th century, boats and aircraft were built out of modern composites produced glass fiber reinforced resins in the 1930s. Application area of composites materials has grown with development of new fiber such as carbon, boron, and aramids, and new composite system with matrices made of metals and ceramics in the 1970s (Kaw, 2006). Figure 2.1 shows the change of relative importance of four major materials, metals, polymers, composite and ceramics on yearly basis. As presented schematically in the chart, the

degreasing role of metals can be seen obvioulsly besides increasing importance of polymers, composites and ceramics (Gibson, 1994).

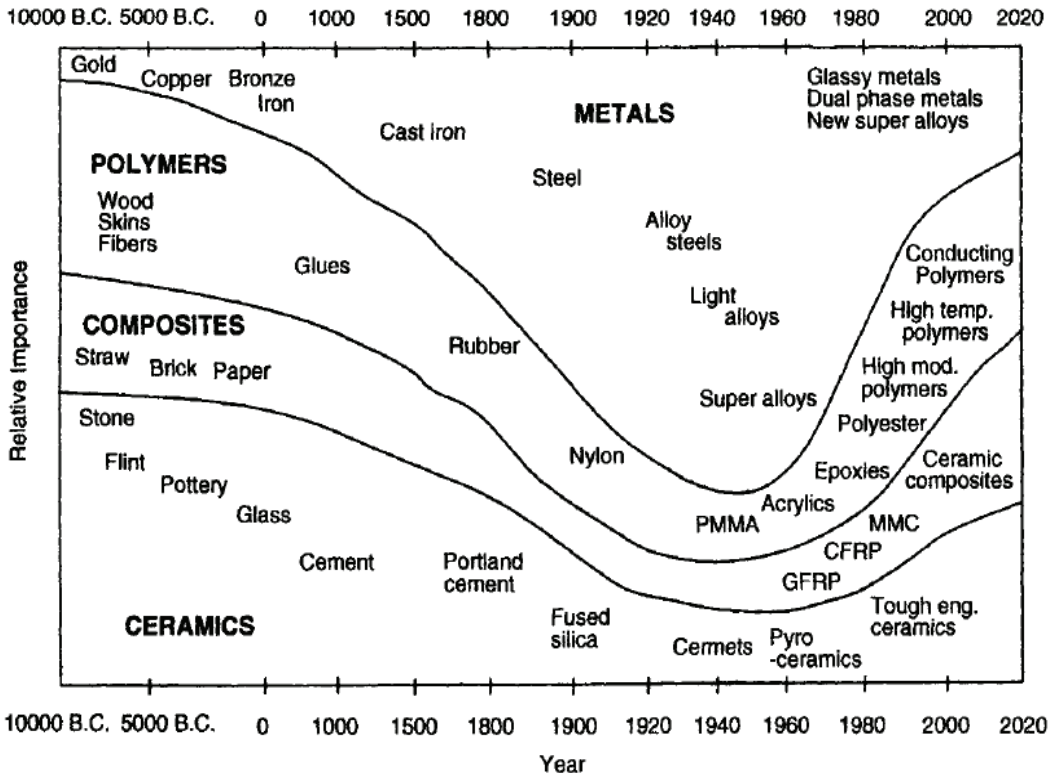

Figure 2.1. Relative importance of material development through history (Source: Ashby, 1987)

The developments in composite materials areas along with their design and manufacturing technologies are one of most significant advances in the history of materials. The main difference of composite structures is that they can be tailored to meet the requirements of a particular application due to the anisotropic nature. When compering with the other many traditional materials, high stiffness (Young's modulus), strength, toughness, great resistance to wear and corrosion, as opposed to their low density, can be counted among the best properties of composite material (see Table 2.1). Fiber reinforced composite materials also have high internal damping, which means that vibrational energy is absorbed within the material, this property plays important role when taking into consideration the structures that are subjected to variable external force. In addition, fatigue strength as well as fatigue damage tolerance of many composite laminates are excellent. For these reasons, fiber reinforced materials have

come up as a major class of structural materials and are either used or being considered for use as substitution for metals in many weight-critical components in aerospace, automotive, and other industries (Mallick, 2007).

Table 2.1. Tensile properties of some metallic and structural composite materials (Source: Mallick, 2007)

Material[a]	Density, g/cm^3	Modulus, GPa (Msi)	Tensile Strength, MPa (ksi)	Yield Strength, MPa (ksi)	Ratio of Modulus to Weight,[b] 10^6 m	Ratio of Tensile Strength to Weight,[b] 10^3 m
SAE 1010 steel (cold-worked)	7.87	207 (30)	365 (53)	303 (44)	2.68	4.72
AISI 4340 steel (quenched and tempered)	7.87	207 (30)	1722 (250)	1515 (220)	2.68	22.3
6061-T6 aluminum alloy	2.70	68.9 (10)	310 (45)	275 (40)	2.60	11.7
7178-T6 aluminum alloy	2.70	68.9 (10)	606 (88)	537 (78)	2.60	22.9
Ti-6A1-4V titanium alloy (aged)	4.43	110 (16)	1171 (170)	1068 (155)	2.53	26.9
17-7 PH stainless steel (aged)	7.87	196 (28.5)	1619 (235)	1515 (220)	2.54	21.0
INCO 718 nickel alloy (aged)	8.2	207 (30)	1399 (203)	1247 (181)	2.57	17.4
High-strength carbon fiber–epoxy matrix (unidirectional)[a]	1.55	137.8 (20)	1550 (225)	—	9.06	101.9
High-modulus carbon fiber–epoxy matrix (unidirectional)	1.63	215 (31.2)	1240 (180)	—	13.44	77.5
E-glass fiber–epoxy matrix (unidirectional)	1.85	39.3 (5.7)	965 (140)	—	2.16	53.2
Kevlar 49 fiber–epoxy matrix (unidirectional)	1.38	75.8 (11)	1378 (200)	—	5.60	101.8
Boron fiber-6061 A1 alloy matrix (annealed)	2.35	220 (32)	1109 (161)	—	9.54	48.1
Carbon fiber–epoxy matrix (quasi-isotropic)	1.55	45.5 (6.6)	579 (84)	—	2.99	38
Sheet-molding compound (SMC) composite (isotropic)	1.87	15.8 (2.3)	164 (23.8)		0.86	8.9

The physical and mechanical properties of composites differ in depending on the properties of constituents, geometry and distribution of the materials. Volume fraction is one of significiant parameters for composite material. It represents the rate of fiber volume into the whole volume of composite material. Fiber volume fraction into composite material might be identified by using standart burn-off technique. The distribution of reinforcement phase defines the homogenity and heterogenity on the macroscopic scale.

The geometry and aspects of fibres (short and endless fibres) determine isotropy or orthotropy properties of material. The material is isotropic if the properties such as stiffness, strength, thermal expansion and conductivty are assumed to be uniform in all directions, otherwise the properties of material that are dependent on the direction are anisotropic. Metals and alloys are example of isotropic material, whereas composite materials exhibit anisotropic behaviour because they have the different properties in all directions.

The kind of fiber-reinforced composites commonly used in structural applications is called a laminate. which is made by stacking a number of thin layers of fibers and matrix and collecting them into the desired thickness. Fiber orientation in each layer as well as the stacking sequence of various layers in a composite laminate can be arranged to achieve a wide range of physical and mechanical properties for the composite laminate (Mallick, 2007). Lamina or Ply is thin single layer of composite material, which is approximately in thickness of 1mm. Composite laminate consist of two or more unidirectional lamina or ply stacked together at various angle, as shown in Figure 2.2.

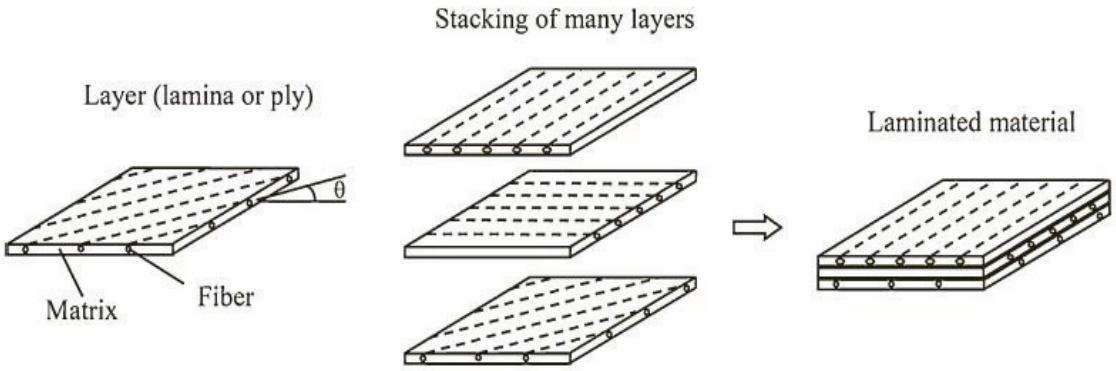

Figure 2.2. Lamina and laminate lay-ups
(Source: Campbell, 2010)

Despite offering the distinct features, composite materials have some limitations or drawbacks when compared to the metals. Some of the disadvantages of composite material include:

- Fabrication cost of composite materials is high.
- Manufacturing and assembly of composites is time-consuming process.
- Mechanical characterization of composite structure is more complex compared to metals.
- Repair procedure of composite material is not easy process according to metal materials.

2.2. Types and Classification of Composite Materials

Composite materials are commonly classified into two major categories according to type of matrix or reinforcement phase. One of classification is usually made as based on matrix constituent used: polymer, metal, ceramic and carbon matrix composites. %30-%40 of composite structure is generally made from the matrix (Akovali, 2001). The matrix phase in composites performs several critical role as well as keeping the fibers in proper oriantation, which provides uniform load distrubution to the reinforcing constituent and also protects the composite surface againts abrasion, mechanical damage and environmental corrosion. Matrix phase has a lower modulus than the fiber so that it strains more.

Polymer Matrix Composites (PMC), which are most populer one due to their low cost and simple fabrication method, consist of thermoset (epoxy, polyimide, polyester) or thermoplastic (poly-ether-ether-ketone, polysulfone) resins combined with a fibrous reinforcing dispersed phase. They are preferred in low temperature applications.

Metal Matrix Composites (MMC) consist of metals and alloy (aluminium, titanium, copper and magnesium) combined with glass, carbon, aramid and boron fibers. MMCs are widely used to provide the advantages over metal. The main advantages of MMCs include higher spesific strength and modulus, lower coefficients of termal expansion, damping capasity along with low density. Their maximum usage temperature is restricted due to the softening or melting temperature of the metal matrix.

Ceramic Matrix Composites (CMC) consist of metallic and non-metallic constutients (silicon carbide, aluminium oxide, glass-ceramic, silicon nitride) combined with ceramic fibers. Important characteristics of ceramic matrix is to have a very high application temperature range. The main disadvantage of which is susceptible to flawing due to brittleness of ceramic materials. On the other side of being brittle, they have low thermal and mechanical shock resistances (Daniel and Ishai, 1994).

Carbon-carbon (C/C) composites consist of carbon fiber reinforcement combined with carbon matrix. Carbon–carbon composites originally have been developed for aerospace applications. They have unique properties such as low density, high thermal conductivity, dimensional stability and excellent mechanical properties.

These types of composites are utilized in very high-temperature environments of up to 3315°C. Carbon is brittle and flaw sensitive like in ceramic materials. The following advantages can be listed forreinforcement of a carbon matrix: (*i*) the composites fail gradually, (*ii*) it increases ability to withstand high temperatures, (*iii*) it provides low creep at high temperatures.

Some of the fiber-matrix combinations of composite materials are shown in Table 2.2.

Table 2.2. Types of laminated composite materials
(Source: Daniel and Ishai, 1994)

Matrix type	Fiber	Matrix
Polymer	E-glass	Epoxy
	S-glass	Polyimide
	Carbon (graphite)	Polyester
	Aramid (Kevlar)	Thermoplastics
	Boron	(PEEK, polysulfone, etc.)
Metal	Boron	Aluminium
	Borsic	Magnesium
	Carbon (graphite)	Titanium
	Silicon carbide	Copper
	Alumina	
Ceramic	Silicon carbide	Silicon carbide
	Alumina	Alumina
	Silicon nitride	Glass-ceramic
		Silicon nitride
Carbon	Carbon	Carbon

The other classification is made according to the type, geomerty and oriantation of reinforcement phase used, is shown in Figure 2.3. Fibers cover the largest volume fraction in a composite laminate and carry the major portion of the load acting on a composite structure. The reinforcement phase in a composite structure may be in the different forms such as discontinuous (either in the form of dispersions/particles, flakes, whiskers, discontinuous short fibres with different aspect ratios) or continuous (long fibres and sheets). Although particulate or fibrous form is the most common in use (Akovali, 2001). It is important to choose proper the fiber type, fiber volume fraction,

fiber length and fiber orientation because they directly affect the following characteristics of a composite laminate (Mallick, 2007):

- Density
- Tensile strength and modulus
- Compressive strength and modulus
- Fatigue strength as well as fatigue failure mechanisms
- Electrical and thermal conductivities
- Cost

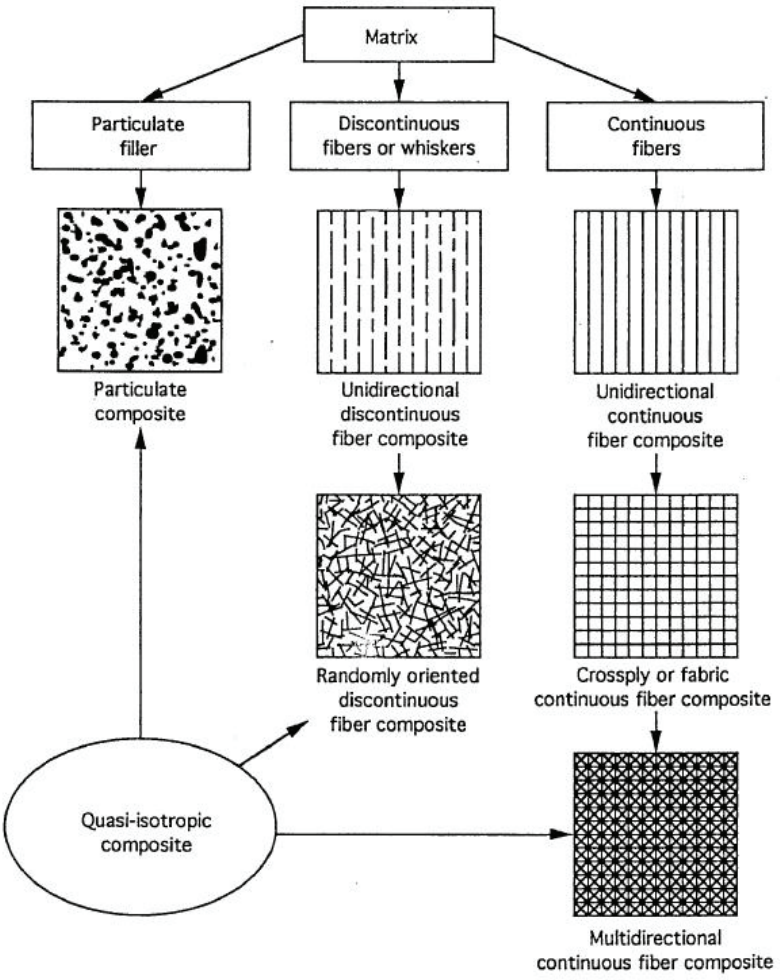

Figure 2.3. Classification of composite materials
(Source: Daniel and Ishai, 1994)

Particulate composite is composed of particles in various size and shapes randomly embedded within the matrix. The size of particulates can be very small (< 0.25 microns). Particles may enhance the some properties of materials such as rigidity, termal behavior, resistance to abrasion and also improve the fracture strength of the composite by preventing crack propagation through the matrix. Particle reinforced composites have low cost and ease of production and forming. Particle reinforced composites are widely used the applications where high levels of wear resistance are required.

Discontinous or short-fiber composites are composites that the reinforcing phase is in the form of short fibers or whiskers. Composites reinforced with discontinous fiber are prefered where the higher strength and stiffness of continous fiber composite are not needed. Discontinous fiber-reinforced composites are attractive due to the low fabrications cost. Since the short fibers disperse randomly within material, composite structure exhibits nearly isotropic behavior.

Continuous fiber composites are composed of axial long continuous fibers embedded in a matrix material. Fiber-reinforced composites are most efficient in terms of stiffness and strength. The orientation angle of continuous fibers may be different. They can be all parallel to each other (unidirectional continuous fiber composite), can be directed at right angles to each other (cross-ply or woven fabric continuous fiber composite), can be directed along many directions (multidirectional continuous fiber composite) (Daniel and Ishai, 1994).

In addition to types discussed above, hybrid composites are new types of composite material contaning the combination of reinforcing layer from two or more types of fiber such as mixed chopped and continouous fibers or mixed fiber types within the polymer single matrix material. The hybrid fiber reinforced composites exhibit superior mechanical, thermal, damping properties compared to single-fiber reinforced composites.

In this thesis, polymer matrix fiber-reinforced composite (graphite/epoxy) is considered as design material.

2.3. Application of Composite Materials

Composites are increasingly used in a wide variety of commercial and industrial applications such as automotive, marine, aircraft, aerospace, satellite, as well as special consumer products like skis, golf clubs and tennis rackets. Nowadays, it is difficult to find any industry that does not research on use of composite materials for their products. Increased strength, durability, corrosion resistance, resistance to fatigue and damage tolerance characteristics, high-temperature strength can be counted as attractive properties of composite materials.

The earliest applications of composite technology have been seen in aerospace sector because of their exceptional strength and stiffness-to-density ratios and superior physical properties. They provide significant weight advantages. It is possible to obtain approximately 20-30 % lighter composite parts compared to conventional metal parts at the present. The lower weight means lower fuel consumption and lower manufacturing costs. The most common fiber types such as glass, carbon, kevlar and their hybrid have been used to manufacture the aerospace parts.

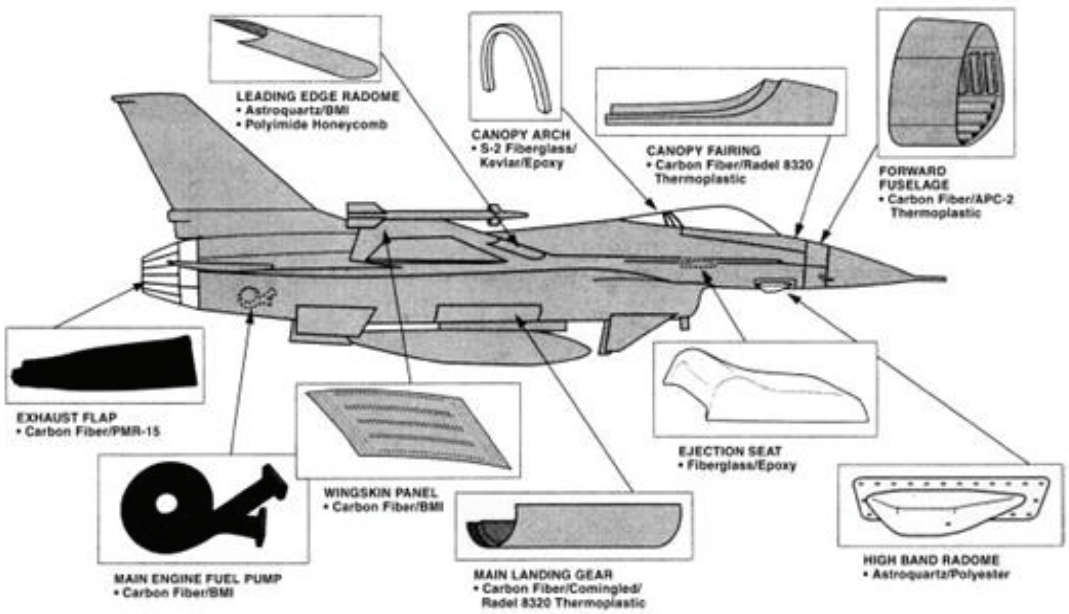

Figure 2.4. Composite components used in military aircraft
(Source: Mazumdar, 2002)

Composites, which were made from glass fibre reinforced plastics, were first introduced by the military aircraft industry in the 1960s. Subsequently, each improved generation of new military aircraft and helicopters has increased usage of composites. Carbon fibers were invented in 1970s and carbon fiber-reinforced epoxy has become very popular due to the several advantages including high stiffness, high chemical resistance, low thermal expansion and indispensable material for wing, fuselage and empennage components. In 1999, the aerospce industry spent 23 milion pounds for composites. Composite materials were mainly used in the models of F-11, F-14, F-15 and F-16 to decrease the weight of structure as shown in Figure 2.4 (Mazumdar, 2002). By the 1980s, composites have been primary part of their design of civil aircraft manufacturers. Composite material usage in Airbus 380 is about %25 of its weight (Mallick, 2007). Satellite structure shown in Figure 2.5 are the other application example of composite materials in aviation sector. The thermo-elastic stability of satellite structure required in orbit can be provided with composite materials.

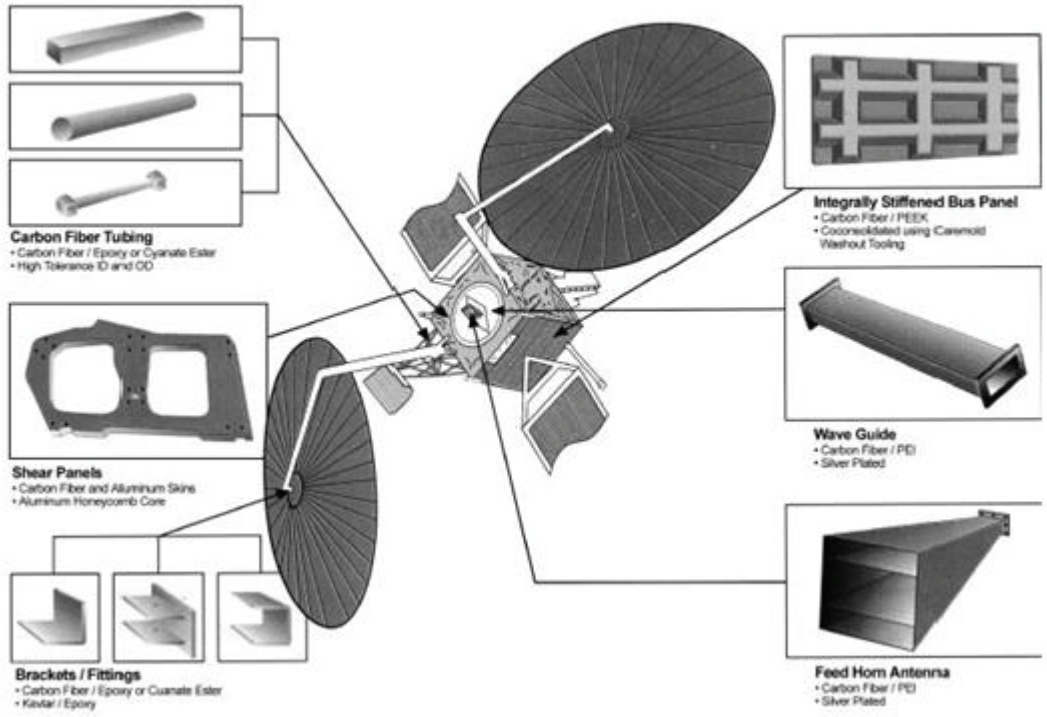

Figure 2.5. Composite components used in satellite components
(Source: Mazumdar, 2002)

Automotive industry is one of the largest market for composite materials. Increased global competition, the need for higher-performance vehicles, a reduction in costs and tighter environmental and safety requirements are challenges of the automotive industry. One of the first and most important factor is the choice of appropriate materials providing the requirements for a vehicle in automotive design. Composite materials satisfy the expectation to overcome these issues (Elmarakbi, 2014). Early application of composite materials seen in the 1953 Corvettes, which were produced with all-fiberglass bodies, is shown in Figure 2.6. Since those early days, composites are attractive alternative to metals and being used increasingly in automotive industry.

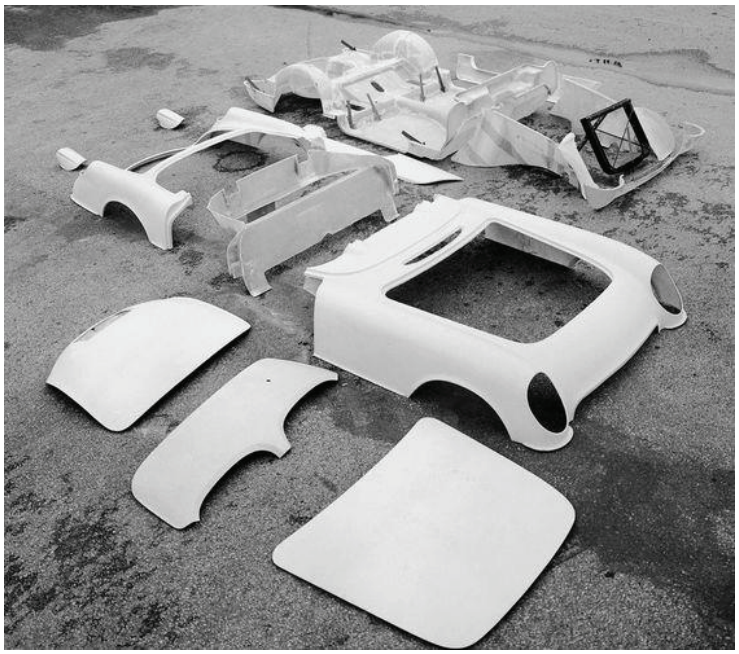

Figure 2.6. First fiberglass corvette body parts
(Source: http://www.moldedfiberglass.com)

Composites have been also used in the production of drive shafts, fan blades, springs, bumpers, interior panel, tires, belts and engine parts.

Athletic and recreational equipments such as tennis rackets, golf clubs, softball bats, hockey sticks, archery arrows and bows, helmets, fishing rods, windsurfing boars are the special consumer products to adopt composite materials. Composites provide excellent combination of easy handling, comfort, lightweight to these products.

CHAPTER 3

MECHANICS OF COMPOSITE MATERIALS

3.1. Introduction

The mechanics of materials is to understand the behavior of solid bodies subjected to various types of loading by considering the concepts of stress, strains, and deformations. The design and analysis of composite material are more complex than conventional materials such as steel and aluminum because conventional materials have homogeneous and isotropic continuity and physical properties of isotropic materials do not vary from point to point on the structure so mechanical properties of an isotropic material are independent of the orientation. Unless metallic materials is severely cold-worked, grains in materials are randomly oriented. Therefore, it is assumed to be isotropic. However, fiber-reinforced composites are microscopically inhomogeneous and nonisotropic (orthotropic) (Mallick, 2007). Composite structures consist of thin single layers bonded each other. Each layer may has different isotropic or orthotropic materials, thicknesses and mechanical properties. The laminate characteristic can be determined by using the information that is related to the number of layers, stacking sequence, geometric and mechanical properties. The inherent characteristics of the constituents, the arrangement and the percentage of reinforcing materials, the fabrication techniques, and the inlife operating temperatures or environmental conditions are factors influencing the mechanical properties of composites. Designers achieved a new flexibility through the use of variables that directly affect the properties of the material along with the introduction of composite materials

The mechanics of fiber-reinforced composite materials are analyzed at two levels: (*i*) macromechanical analysis, (*ii*) micromechanical analysis. A schematic diagram of the various levels of consideration and corresponding types of analysis are shown in Figure 3.1.

Micromechanics: Mechanical analysis of the interactions of the constituents materials is made on a microscopic level. The state of the stress and deformation in the constituents such as matrix failure (tensile, compressive, shear), fiber failure (tensile,

buckling, splitting) and interface failure (debonding), fracture toughness, fatigue life are investigated by using this analysis method.

Macromechanics: An analysis in the macromechanics level is conducted for the interactions of the individual layers of a laminate. The material considers to be homogenous at this level. Material properties of the lamina is averaged value of constituent materials. Failure criteria is predicted by analyzing on macromechanics level.

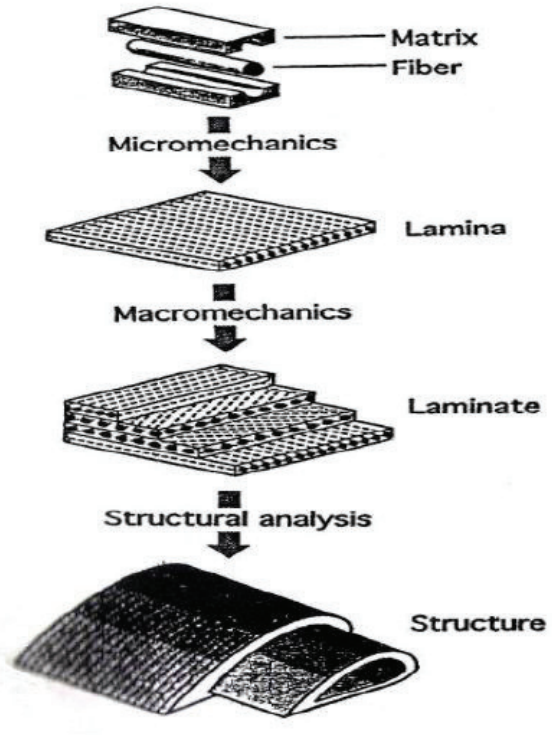

Figure 3.1. Levels of observation and types of analysis for composite materials (Source: Daniel and Ishai 1994)

3.2. Classical Lamination Theory

Classical Laminate Theory (CLT) is extension of the classical plate theory proposed by Kirchhoff –Love and only valid for thin laminates (span a and $b > 10 \times$ thinckness t) with small displacement w in the transverse direction ($w << t$). In this theory, it is assumed that laminate is thin and wide, perfect bounding exists between laminas, there exist a linear strain distribution through the thickness, all laminas are

macroscopically homogeneous and behave in a linearly elastic manner. The thickness strains and transverse shear strains are zero (Kaw 2006).

Figure 3.2. shows thin laminated composite structure subjected to mechanical in plane loading (N_x, N_y). Cartesian coordinate system x, y and z denotes global coordinates of the layered composite material. A layer-wise principal material coordinate system is defined by 1, 2 and 3. Fiber oriantation is directed to the x axis at angle θ.

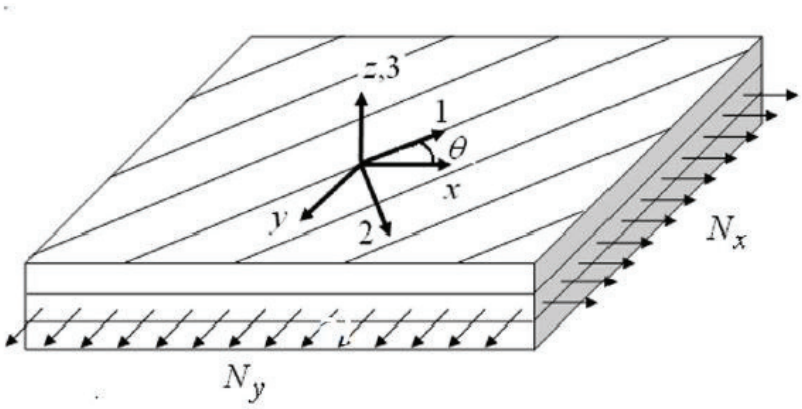

Figure 3.2. A thin fiber-reinforced laminated composite subjected to in plane loading (Source: Aydın and Artem, 2011)

Representation of laminate consisting of N layers with total thickness h is given in Figure 3.3.

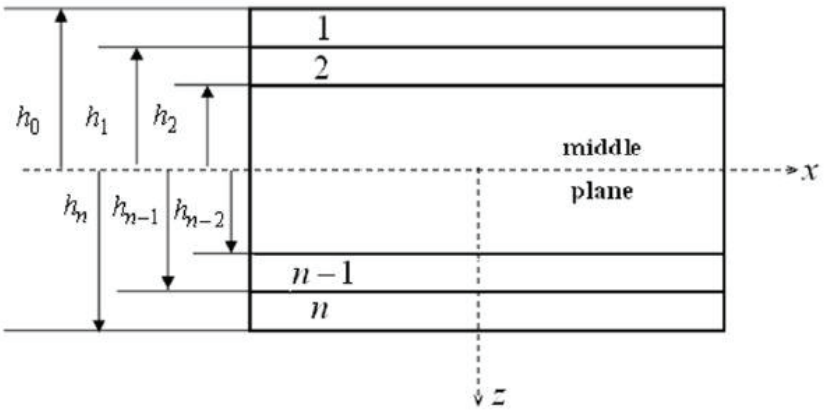

Figure 3.3. Coordinate locations of plies in a laminate (Source: Aydın and Artem, 2011)

The strains at any point in the laminate to the reference plane can be written as

$$\begin{bmatrix} \varepsilon_x \\ \varepsilon_y \\ \gamma_s \end{bmatrix} = \begin{bmatrix} \varepsilon_x^0 \\ \varepsilon_y^0 \\ \gamma_s^0 \end{bmatrix} + z \begin{bmatrix} \kappa_x \\ \kappa_y \\ \kappa_s \end{bmatrix} \tag{3.1}$$

The relation between stress-strain components for the k -th layer of a composite plate based on the classical lamination theory will be in the following form:

$$\begin{bmatrix} \sigma_x \\ \sigma_y \\ \sigma_{xy} \end{bmatrix}_k = \begin{bmatrix} \overline{Q_{11}} & \overline{Q_{12}} & \overline{Q_{16}} \\ \overline{Q_{12}} & \overline{Q_{22}} & \overline{Q_{26}} \\ \overline{Q_{16}} & \overline{Q_{26}} & \overline{Q_{66}} \end{bmatrix}_k \left(\begin{bmatrix} \varepsilon_x{}^\circ \\ \varepsilon_y{}^\circ \\ \varepsilon_{xy}{}^\circ \end{bmatrix} + z \begin{bmatrix} \kappa_x \\ \kappa_y \\ \kappa_{xy} \end{bmatrix} \right) \tag{3.2}$$

where $\left[\overline{Q_{ij}}\right]_k$ are the elements of the transformed reduced stiffness matrix, $\left[\varepsilon^\circ\right]$ is the mid-plane strains, $\left[\kappa\right]$ is curvatures, respectively. The coordinate transformation matrix $\left[T\right]$ is defined to express the relation between principal axes (1, 2) and reference axes (x, y), is written in the following matrix form:

$$\left[T\right] = \begin{bmatrix} c^2 & s^2 & 2sc \\ s^2 & c^2 & -2sc \\ -sc & sc & c^2 - s^2 \end{bmatrix} \quad c = \cos\theta\,,\ s = \sin\theta \tag{3.3}$$

The elements of the transformed reduced stiffness matrix $\left[\overline{Q_{ij}}\right]_k$ appearing in Equation 3.2 can be defined as in the following form:

$$\overline{Q}_{11} = Q_{11}c^4 + Q_{22}s^4 + 2(Q_{12} + 2Q_{66})s^2c^2 \tag{3.4}$$

$$\overline{Q}_{12} = (Q_{11} + Q_{22} - 4Q_{66})s^2c^2 + Q_{12}(c^4 + s^4) \tag{3.5}$$

$$\overline{Q}_{22} = Q_{11}s^4 + Q_{22}c^4 + 2(Q_{12} + 2Q_{66})s^2c^2 \tag{3.6}$$

$$\overline{Q}_{16} = (Q_{11} - Q_{12} - 2Q_{66})sc^3 - (Q_{22} - Q_{12} - 2Q_{66})s^3c \tag{3.7}$$

$$\overline{Q}_{26} = (Q_{11} - Q_{12} - 2Q_{66})cs^3 - (Q_{22} - Q_{12} - 2Q_{66})sc^3 \tag{3.8}$$

$$\overline{Q}_{66} = (Q_{11} + Q_{22} - 2Q_{12} - 2Q_{66})s^2c^2 + Q_{66}(c^4 + s^4) \tag{3.9}$$

where stiffness matrix quantities $\left[Q_{ij}\right]$ are

$$Q_{11} = \frac{E_1}{1 - \nu_{21}\nu_{12}} \tag{3.10}$$

$$Q_{12} = \frac{\nu_{12}E_2}{1 - \nu_{21}\nu_{12}} \tag{3.11}$$

$$Q_{22} = \frac{E_2}{1 - \nu_{21}\nu_{12}} \tag{3.12}$$

$$Q_{66} = G_{12} \tag{3.13}$$

The principal stiffness terms, Q_{ij}, depending on elastic properties of the material along the principal directions, E_1, E_2, G_{12}, υ_{12} and υ_{21}. The in-plane loads (N_x, N_y and N_{xy}) and the moments (M_x, M_y, M_{xy}) in general have the following relations:

$$\begin{bmatrix} N_x \\ N_y \\ N_{xy} \end{bmatrix} = \begin{bmatrix} A_{11} & A_{12} & A_{16} \\ A_{12} & A_{22} & A_{26} \\ A_{16} & A_{26} & A_{66} \end{bmatrix} \begin{bmatrix} \varepsilon_x^\circ \\ \varepsilon_y^\circ \\ \gamma_{xy}^\circ \end{bmatrix} + \begin{bmatrix} B_{11} & B_{12} & B_{16} \\ B_{12} & B_{22} & B_{26} \\ B_{16} & B_{26} & B_{66} \end{bmatrix} \begin{bmatrix} \kappa_x \\ \kappa_y \\ \kappa_{xy} \end{bmatrix} \tag{3.14}$$

$$\begin{bmatrix} M_x \\ M_y \\ M_{xy} \end{bmatrix} = \begin{bmatrix} B_{11} & B_{12} & B_{16} \\ B_{12} & B_{22} & B_{26} \\ B_{16} & B_{26} & B_{66} \end{bmatrix} \begin{bmatrix} \varepsilon_x^\circ \\ \varepsilon_y^\circ \\ \gamma_{xy}^\circ \end{bmatrix} + \begin{bmatrix} D_{11} & D_{12} & D_{16} \\ D_{12} & D_{22} & D_{26} \\ D_{16} & D_{26} & D_{66} \end{bmatrix} \begin{bmatrix} \kappa_x \\ \kappa_y \\ \kappa_{xy} \end{bmatrix} \tag{3.15}$$

The matrices [A], [B] and [D] given in Equation 3.14 and 3.15 are extensional stiffness, coupling stiffness and bending laminate stiffness, respectively. These matrices can be defined as

$$A_{ij} = \sum_{k=1}^{n} (\overline{Q_{ij}})^k (h_k - h_{k-1}) \tag{3.16}$$

$$B_{ij} = \frac{1}{2} \sum_{k=1}^{n} (\overline{Q_{ij}})^k ({h^2}_k - {h^2}_{k-1}) \tag{3.17}$$

$$D_{ij} = \frac{1}{2} \sum_{k=1}^{n} (\overline{Q_{ij}})^k ({h^3}_k - {h^3}_{k-1}) \tag{3.18}$$

There is no coupling between in-plane loading and out of plane deformation for symmetric laminates. Therefore, the coupling stiffness matrix (B_{ij}) is equal to zero. The load-deformations relations can be reduced to

$$\begin{bmatrix} N_x \\ N_y \\ N_{xy} \end{bmatrix} = \begin{bmatrix} A_{11} & A_{12} & A_{16} \\ A_{12} & A_{22} & A_{26} \\ A_{16} & A_{26} & A_{66} \end{bmatrix} \begin{bmatrix} \varepsilon_x^{\circ} \\ \varepsilon_y^{\circ} \\ \gamma_{xy}^{\circ} \end{bmatrix} \tag{3.19}$$

$$\begin{bmatrix} M_x \\ M_y \\ M_{xy} \end{bmatrix} = \begin{bmatrix} D_{11} & D_{12} & D_{16} \\ D_{12} & D_{22} & D_{26} \\ D_{16} & D_{26} & D_{66} \end{bmatrix} \begin{bmatrix} \kappa_x \\ \kappa_y \\ \kappa_{xy} \end{bmatrix} \tag{3.20}$$

The extension stiffness matrix [A] relates the resultant in-plane forces to the in-plane strains, and the bending stiffness matrix [D] relates the resultant bending moments to the plate curvature. The coupling stiffness matrix [B] couples the force and moment to the mid-plane strains and mid-plane curvatures (Kaw, 2006).

The relation between stresses and strain based on classical lamination theory can be expressed in local coordinate system (1, 2). The transformation matrix of the local and global stresses in angled lamina can be described as follows:

$$\begin{bmatrix} \sigma_1 \\ \sigma_2 \\ \sigma_{12} \end{bmatrix} = [\mathrm{T}] \begin{bmatrix} \sigma_x \\ \sigma_y \\ \sigma_{xy} \end{bmatrix} \tag{3.21}$$

Similarly, the local and global strains are written as follows:

$$\begin{bmatrix} \varepsilon_1 \\ \varepsilon_2 \\ \varepsilon_{12} \end{bmatrix} = [\mathrm{R}][\mathrm{T}][\mathrm{R}]^{-1} \begin{bmatrix} \varepsilon_x \\ \varepsilon_y \\ \varepsilon_{xy} \end{bmatrix} \tag{3.22}$$

where

$$[R] = \begin{bmatrix} 1 & 0 & 0 \\ 0 & 1 & 0 \\ 0 & 0 & 2 \end{bmatrix} \tag{3.23}$$

3.3. Vibration Analysis of Laminated Composite Plate

Vibration is one of the most critical phenomena for mechanical structures. The knowledge of vibration characteristics is important for the predesign of the engineering structures. Vibration directly affects the performance and life of them. In general, the analysis for the vibration problem of the rectangular plates has been done based on the classical thin plate theory. The analytic expressions for a rectangular plate can be solved by using Navier solution technique when all four edges of the laminate are simply

supported. On the other hand, plate structures may be found in different edge constraints under its working conditions. The Rayleigh-Ritz energy method offers the approximate solution to determine the natural frequencies of laminated composite plate under more general boundary conditions, as long as suitable approximation functions can be found the problem. The method is dependent upon the approximation functions chosen for the dynamic deflection curves.

3.3.1. All Sides Simply Supported

It is assumed that the plate is a rectangular with dimensions of L_x and L_y, which has simply supported boundary conditions along its four edges. The deflection of the plate under free and undamped vibration is sinusoidal with respect to time t

$$w^\circ = \overline{w}^\circ \sin(\omega t) = \overline{w}^\circ \sin(2\pi f t) \tag{3.24}$$

where ω and f are circular frequency and natural frequency, respectively. The period of vibration T is as follow. $\overline{w}^\circ$ is the maximum amplitude of the plate at time $t = \frac{T}{4}$.

$$T = \frac{1}{f} \qquad \omega = 2\pi f = \frac{2\pi}{T}, \tag{3.25}$$

The curvatures of plane are

$$\kappa_x = -\frac{\partial^2 \omega^\circ}{\partial x^2}, \qquad \kappa_y = -\frac{\partial^2 \omega^\circ}{\partial y^2}, \qquad \kappa_{xy} = -\frac{2\partial^2 \omega^\circ}{\partial x \partial y} \tag{3.26}$$

Strain energy for linearly elastic material under the plane stress conditions ($\sigma_z = 0$, $\tau_{xz} = 0$ and $\tau_{yz} = 0$) is expressed as

$$U = \frac{1}{2}\int_0^{L_x}\int_0^{L_y} \begin{bmatrix} \varepsilon_x \\ \varepsilon_y \\ \gamma_{xy} \\ \kappa_x \\ \kappa_y \\ \kappa_{xy} \end{bmatrix}^T \begin{bmatrix} A_{11} & A_{12} & A_{16} & B_{11} & B_{12} & B_{16} \\ A_{12} & A_{22} & A_{26} & B_{12} & B_{22} & B_{26} \\ A_{16} & A_{26} & A_{66} & B_{16} & B_{26} & B_{66} \\ B_{11} & B_{12} & B_{16} & D_{11} & D_{12} & D_{16} \\ B_{12} & B_{22} & B_{26} & D_{12} & D_{22} & D_{26} \\ B_{16} & B_{26} & B_{66} & D_{16} & D_{26} & D_{66} \end{bmatrix} \begin{bmatrix} \varepsilon_x \\ \varepsilon_y \\ \gamma_{xy} \\ \kappa_x \\ \kappa_y \\ \kappa_{xy} \end{bmatrix} dydx \tag{3.27}$$

Laminated composite plates are symmetrical with respect to mid-plane (i.e., $[B]=0$) and the in-plane strains in mid-plane are zero ($\varepsilon_x = \varepsilon_y = \gamma_{xy} = 0$), strain energy simplifies to

$$U = \frac{1}{2}\int_0^{L_x}\int_0^{L_y} \begin{bmatrix} \kappa_x & \kappa_y & \kappa_{xy} \end{bmatrix} \begin{bmatrix} D_{11} & D_{12} & D_{16} \\ D_{12} & D_{22} & D_{26} \\ D_{16} & D_{26} & D_{66} \end{bmatrix} \begin{bmatrix} \kappa_x \\ \kappa_y \\ \kappa_{xy} \end{bmatrix} dydx \tag{3.28}$$

After adding the strains and curvatures terms into strain energy expression (U), one gets

$$U = \overline{U}\sin^2(2\pi ft) \tag{3.29}$$

where $\overline{U}$ is defined as

$$\overline{U} = \frac{1}{2}\int_0^{L_x}\int_0^{L_y} \left[D_{11}\left(\frac{\partial^2 \overline{w}^\circ}{\partial x^2}\right)^2 + D_{22}\left(\frac{\partial^2 \overline{w}^\circ}{\partial y^2}\right)^2 + D_{66}\left(\frac{2\,\partial^2 \overline{w}^\circ}{\partial x\,\partial y}\right)^2 \right.$$

$$\left. + 2\left(D_{12}\frac{\partial^2 \overline{w}^\circ}{\partial x^2}\frac{\partial^2 \overline{w}^\circ}{\partial y^2} + D_{16}\frac{\partial^2 \overline{w}^\circ}{\partial x^2}\frac{2\,\partial^2 \overline{w}^\circ}{\partial x\,\partial y} + D_{26}\frac{\partial^2 \overline{w}^\circ}{\partial y^2}\frac{2\,\partial^2 \overline{w}^\circ}{\partial x\,\partial y} \right) \right] dydx \tag{3.30}$$

The kinetic energy of the plate is also defined as

$$K = \frac{1}{2}\int_0^{L_x}\int_0^{L_y} \rho\left(\frac{dw^\circ}{dt}\right)^2 dydx \tag{3.31}$$

Substitution of the deflection given by Equation 3.24 into Equation 3.31 yields

$$K = \frac{1}{2}(2\pi f)^2 \cos^2(2\pi f\, t)\int_0^{L_x}\int_0^{L_y} \rho\overline{w^\circ}^2 dydx \tag{3.32}$$

The changes in strain energy and kinetic energy from time t=0 to time t is equal to each other according to the law of conservation of energy:

$$(U_t - U_{t=0}) = -(\mathrm{K_t} - K_{t=0}) \tag{3.33}$$

At the beginning, the strain energy is zero at t=0 (Equation 3.29). However, the kinetic energy is zero at time $t = \frac{1}{4f}$ (Equation 3.32). Thus, one has

$$U_{t=\frac{1}{4f}} = K_{t=0} \tag{3.34}$$

Equation 3.34, together with Equations 3.29 and 3.32, yields

$$\frac{1}{2}(2\pi f)^2 \int_0^{L_x}\int_0^{L_y} \rho\overline{w}^{\circ 2}\, dy\, dx = \overline{U} \tag{3.35}$$

From this equation, one has

$$(2\pi f)^2 = \frac{\overline{U}}{\frac{1}{2}\int_0^{L_x}\int_0^{L_y} \rho\overline{w}^{\circ 2}\, dy\, dx} \tag{3.36}$$

The Rayleigh Ritz method is used to obtain the deflection. For the simply supported plate under consideration the geometrical boundary conditions require that the deflections are zero along the edges as follows:

$$\overline{w}^{\circ} = 0 \quad \text{at} \quad \begin{Bmatrix} x = 0 & and & 0 \le y \le L_y \\ x = L_x & and & 0 \le y \le L_y \\ 0 \le x \le L_x & and & y = 0 \\ 0 \le x \le L_x & and & y = L_y \end{Bmatrix} \tag{3.37}$$

The following function for deflection satisfies these geometrical boundary conditions (Equation 3.37):

$$w^{\circ} = \overline{w}^{\circ} \sin(2\pi ft) \tag{3.38}$$

where $\overline{w}^{\circ}$ is

$$\overline{w}^{\circ} = \sum_{i=1}^{I} \sum_{j=1}^{J} w_{ij} \sin \frac{i\pi x}{L_x} \sin \frac{j\pi y}{L_y} \tag{3.39}$$

where I and J are the number of the terms chosen arbitrarily and w_{ij} is constants. The variables *i* and *j* represents the number of half waves in the x and y directions, respectively. The frequency of vibration of a conservative system has a minimum value in the neighborhood of the fundamental mode according to the Rayleigh principle (Kollar and Springer, 2003). One expresses this principle in the form

$$\frac{\partial f}{\partial w_{ij}} = 0 \tag{3.40}$$

The values of w_{ij} are determined by substituting Equations 3.30, 3.36 and 3.39 into the following expression. Algebraic manipulations yield the following system of simultaneous algebraic equations:

$$\sum_{i=1}^{I}\sum_{j=1}^{J}(G_{mnij}-\lambda\delta_{mnij})\,\mathrm{w_{ij}}=0 \qquad \left\{\begin{matrix} i,m=1,2,3.....,I \\ j,n=1,2,3.....,\mathrm{J}\end{matrix}\right\} \tag{3.41}$$

where λ is given by

$$\lambda=\frac{1}{4}(2\pi f)^2\rho L_x L_y \tag{3.42}$$

For convenience, the contracted notation is introduced

$$\begin{aligned} k&=(i-1)J+j \quad \left\{\begin{matrix} i=1,2,3.....I \\ j=1,2,3,...J\end{matrix}\right\} \\ I&=(m-1)J+n\left\{\begin{matrix} m=1,2,3,...I \\ n=1,2,33...J\end{matrix}\right\} \end{aligned} \tag{3.43}$$

Equation 3.41 may now be written as

$$\sum_{k=1}^{IxJ}G_{kl}w_k=\lambda\sum_{k=1}^{IxJ}\delta_{kl}w_k \qquad k,l=1,2,3.....IxJ \tag{3.44}$$

where $G_{kl}\,(=G_{lk})$ and the Kronecker delta $\delta_{kl}\;(=\delta_{lk})$ are given in Table 3.1.

Table 3.1. The elements of the matrix [G]
(Source: Kollar and Springer, 2003)

$$G_{lk} = \frac{1}{4} L_x L_y \pi^4 \left[D_{11} \left(\frac{i}{L_x} \right)^4 + 2\left(D_{12} + 2D_{66} \right) \left(\frac{i}{L_x} \right)^2 \left(\frac{i}{L_y} \right)^2 + D_{22} \left(\frac{i}{L_y} \right)^4 \right] \delta_{lk}$$

$$-2L_x L_y \pi^4 D_{16} \left[\left(\frac{i}{L_x} \right)^2 \left(\frac{m}{L_x} \right) \left(\frac{n}{L_y} \right) r_{im}\, r_{jn} + \left(\frac{m}{L_x} \right)^2 \left(\frac{i}{L_x} \right) \left(\frac{i}{L_y} \right) r_{mi}\, r_{nj} \right]$$

$$-2L_x L_y \pi^4 D_{26} \left[\left(\frac{i}{L_y} \right)^2 \left(\frac{m}{L_x} \right) \left(\frac{n}{L_y} \right) r_{im}\, r_{jn} + \left(\frac{n}{L_y} \right)^2 \left(\frac{i}{L_x} \right) \left(\frac{i}{L_y} \right) r_{mi}\, r_{nj} \right]$$

$$\delta_{lk} = \begin{cases} 1 \rightarrow k = l \\ 0 \rightarrow k \neq l \end{cases} \qquad r_{ij} = \begin{cases} \dfrac{2i}{(i^2 - j^2)\pi} & \rightarrow (\mathrm{i} - \mathrm{j}) = odd \\ 0 & \rightarrow (\mathrm{i} - \mathrm{j}) = even \end{cases}$$

$$k = (i-1)J + j \qquad \begin{cases} i = 1, 2, 3, ..., I \\ j = 1, 2, 3, ..., \mathrm{J} \end{cases}$$

$$l = (m-1)J + n \qquad \begin{cases} m = 1, 2, 3, ..., I \\ n = 1, 2, 3, ..., \mathrm{J} \end{cases}$$

In the expanded form Equation 3.44 is

$$\left[\begin{pmatrix} G_{11} & \cdots & G_{1(IxJ)} \\ \vdots & \ddots & \vdots \\ G_{(IxJ)1} & \cdots & G_{(IxJ)(IxJ)} \end{pmatrix} - \lambda \begin{pmatrix} \delta_{11} & \cdots & \delta_{1(IxJ)} \\ \vdots & \ddots & \vdots \\ \delta_{(IxJ)1} & \cdots & \delta_{(IxJ)(IxJ)} \end{pmatrix} \right] \begin{Bmatrix} w_1 \\ \vdots \\ w_{(IxJ)} \end{Bmatrix} = \begin{Bmatrix} 0 \\ \vdots \\ 0 \end{Bmatrix} \qquad (3.45)$$

The deflection cannot be zero in case of free vibration. Therefore, the determinant of the matrix within the parentheses must be zero. λ is eigenvalue of Equation 3.45 at this condition.

The natural frequencies can be computed from Equation 3.42 as follow:

$$f_{ij} = \frac{1}{\pi}\sqrt{\frac{\lambda_{ij}}{\rho L_x L_y}} \tag{3.46}$$

For an orthotropic plate $D_{16} = D_{26} = 0$, and the eigenvalues of Equation 3.45 can directly be calculated. The result is

$$\lambda_{ij} = \frac{1}{4} L_x L_y \pi^4 \left[D_{11}\left(\frac{i}{L_x}\right)^4 + 2\left(D_{12} + 2D_{66}\right)\left(\frac{i}{L_x}\right)^2\left(\frac{j}{L_y}\right)^2 + D_{22}\left(\frac{j}{L_y}\right)^4 \right] \tag{3.47}$$

Equations 3.46 and 3.47 give the natural frequencies of an orthotropic plate as follow and f_{ij} can be calculated for different values of *i* and *j* (Kollar and Springer, 2003).

$$f_{ij} = \frac{\pi}{2\sqrt{\rho}}\left[D_{11}\left(\frac{i}{L_x}\right)^4 + 2\left(D_{12} + 2D_{66}\right)\left(\frac{i}{L_x}\right)^2\left(\frac{j}{L_y}\right)^2 + D_{22}\left(\frac{j}{L_y}\right)^4 \right]^{1/2} \tag{3.48}$$

3.3.2. Different Boundary Conditions

The general equation of laminated composite plates for free vibration can be obtained by following the steps given in Section 3.3.1. Accordingly, one arrives at

$$(2\pi f)^2 = \frac{\overline{U}}{\frac{1}{2}\int_0^{L_x}\int_0^{L_y} \rho \overline{w}^{\circ 2}\, dy\, dx} \tag{3.49}$$

The deflection is assumed to be of the form

$$\overline{w}^{\circ} = A X_i(x) Y_j(\mathrm{y}) \tag{3.50}$$

where A is the amplitude that is unknown yet. For $X_i(x)$ and $Y_j(y)$, one should adopt the shape of a freely vibrating plate. These functions for different end supports are given in Table 3.2. Consequently, the natural frequencies of the laminated composite plates for different boundary conditions have been calculated by using the following equation (Blevins, 1979).

$$f_{ij} = \frac{\pi}{2\sqrt{\rho}}\left[D_{11}\left(\frac{G_i}{L_x}\right)^4 + 2\left(D_{12}+2D_{66}\right)\frac{H_i}{L_x^{\,2}}\frac{H_j}{L_y^{\,2}} + D_{22}\left(\frac{G_j}{L_y}\right)^4 + \frac{4D_{66}(J_iJ_j - H_iH_j)}{L_x^{\,2}L_y^{\,2}}\right]^{1/2} \tag{3.51}$$

$$i = 1,2,3..., \qquad j = 1,2,3...,$$

where ρ is the mass of per unit area. The dimensionless parameters G, H and J are functions of mode index values *i* and *j* chosen according to type of boundary conditions. The mode index *i* is boundary conditions applied to sides of length b. The mode index *j* is boundary conditions applied to sides of length a. When Figure 3.4. is taken into considiration, simply supported-simply supported boundary conditions, which are on opposite edges, are composed of mode index *i.* For these boundary conditions, G, H and J values are taken as 1 from Table 3.3. Similarly, free-clamped boundary conditions are composed of mode index *j.* For these boundary conditions, G, H and J values are taken as 0.597, -0.0870, 0.471, respectively. These values are for mode index 1 (first mode).

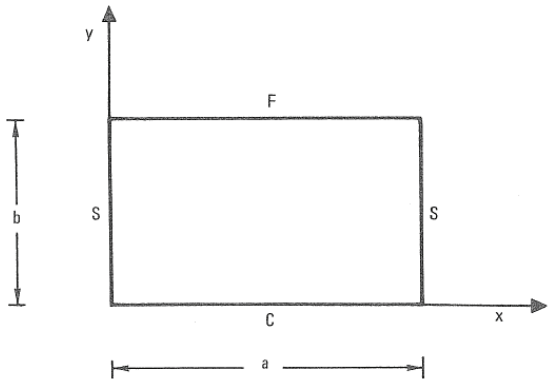

Figure 3.4. Coordinate system for rectangular plate
(Source: Blevins, 1979)

Table 3.2. Displacement function of a freely vibrating plates
(Source: Blevins, 1979)

Boundary Conditions on Opposite Edges	$\lambda_i, i = 1,2,3,$	Displacement function	$\sigma_i, i = 1,2,3,$
1-Free-Free 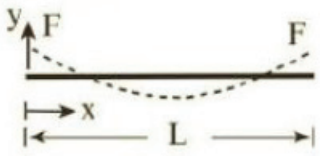	4.73004070 7.85320462 10.9956078 14.1371635 17.2787597 $(2i+1)\pi/2,$ $i>5$	$\cosh\frac{\lambda_i x}{L}+\cos\frac{\lambda_i x}{L}-$ $\sigma_i\left(\sinh\frac{\lambda_i x}{L}+\sin\frac{\lambda_i x}{L}\right)$ $\approx 2.16\left[1-\frac{3}{2}\sin\frac{\pi x}{L}\right],$ $for\ i=1$	0.982502215 1.000777312 0.999966450 1.000001450 $\approx 1 \quad i>5$
2-Simply Supported – Free 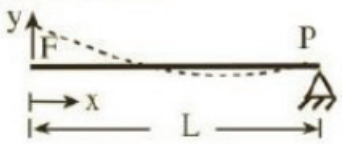	3.92660231 7.06858275 10.21017612 13.35176878 16.49336143 $(4i+1)\pi/4,$ $i>5$	$\cosh\frac{\lambda_i x}{L}+\cos\frac{\lambda_i x}{L}-$ $\sigma_i\left(\sinh\frac{\lambda_i x}{L}+\sin\frac{\lambda_i x}{L}\right)$ $\approx 2.1\left[1-\cos(\pi x/2L)\right],$ $for\ i=1$	1.000777304 1.000001445 1.000000000 1.000000000 $\approx 1 \quad i>5$
3-Clamped – Free 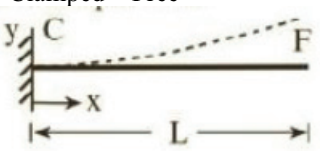	1.87510407 4.69409113 7.85475744 10.99554073 14.13716839 $(2i-1)\pi/2,$ $i>5$	$\cosh\frac{\lambda_i x}{L}-\cos\frac{\lambda_i x}{L}-$ $\sigma_i\left(\sinh\frac{\lambda_i x}{L}+\sin\frac{\lambda_i x}{L}\right)$ $\approx 2.1\left[1-\cos(\pi x/2L)\right],\ for\ i=1$	0.734095514 1.018467319 0.999966450 1.000001450 $\approx 1 \quad i>5$
4-Simply Supported – Simply Supported 	$i\pi,$ $i=1,2,3,..$	$\sin\frac{i\pi x}{L}$	
5-Clamped – Simply Supported 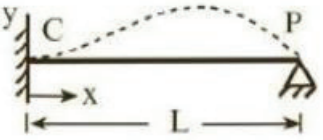	3.92660231 7.06858275 10.21017612 13.35176878 16.49336143 $(4i+1)\pi/4,$ $i>5$	$\cosh\frac{\lambda_i x}{L}-\cos\frac{\lambda_i x}{L}-$ $\sigma_i\left(\sinh\frac{\lambda_i x}{L}+\sin\frac{\lambda_i x}{L}\right)$ $\approx 105^{1/2}\left[\frac{x^2}{L^2}-\frac{x^3}{L^3}\right],\ for\ i=1$	1.000777304 1.000001445 1.000000000 $\approx 1 \quad i>3$
6- Clamped – Clamped 	4.73004070 7.85320462 10.9956078 14.1371635 17.2787597 $(2i-1)\pi/2,$ $i>5$	$\cosh\frac{\lambda_i x}{L}-\cos\frac{\lambda_i x}{L}-$ $\sigma_i\left(\sinh\frac{\lambda_i x}{L}+\sin\frac{\lambda_i x}{L}\right)$ $\approx \sqrt{\frac{2}{3}}\left[1-\cos\frac{2\pi x}{L}\right],\ for\ i=1$	0.982502215 1.000777312 0.999966450 1.000001450 $\approx 1 \quad i>5$

Table 3.3. Coefficients for orthotropic rectangular plates
(Source: Blevins, 1979)

Boundary Conditions on Opposite Edges	Mode Index	G	H	J
1-Free-Free	1 2 3 $n(n>3)$	0 0 1.506 $n-\frac{3}{2}$	0 0 1.248 $\left(n-\frac{3}{2}\right)\left[1-\frac{2}{\left(n-\frac{3}{2}\right)\pi}\right]$	0 1.216 5.017 $\left(n-\frac{3}{2}\right)^2\left[1+\frac{6}{\left(n-\frac{3}{2}\right)\pi}\right]$
2-Simply Supported - Free	1 2 3 $n(n>1)$	0 1.25 2.25 $n-\frac{3}{4}$	0 1.165 4.346 $\left(n-\frac{3}{4}\right)^2\left[1-\frac{1}{\left(n-\frac{3}{4}\right)\pi}\right]$	0.3040 2.756 7.211 $\left(n-\frac{3}{4}\right)^2\left[1+\frac{3}{\left(n-\frac{3}{4}\right)\pi}\right]$
3-Clamped - Free	1 2 3 $n(n>2)$	0.597 1.494 2.500 $n-\frac{1}{2}$	-0.0870 1.347 4.658 $\left(n-\frac{1}{2}\right)^2\left[1-\frac{2}{\left(n-\frac{1}{2}\right)\pi}\right]$	0.471 3.284 7.842 $\left(n-\frac{1}{2}\right)^2\left[1+\frac{2}{\left(n-\frac{1}{2}\right)\pi}\right]$
4-Simply Supported – Simply Supported	1 2 3 n	1 2 3 n	1 4 9 n^2	J = H
5-Clamped – Simply Supported	1 2 3 n	1.25 2.25 3.25 $n+\frac{1}{4}$	1.165 4.346 9.528 $\left(n+\frac{1}{4}\right)^2\left[1-\frac{1}{\left(n+\frac{1}{4}\right)\pi}\right]$	J = H
6- Clamped - Clamped	1 2 3 $n(n>1)$	1.506 2.5 3.5 $n+\frac{1}{2}$	1.248 4.658 10.02 $\left(n+\frac{1}{2}\right)^2\left[1-\frac{2}{\left(n+\frac{1}{2}\right)\pi}\right]$	J = H

In this study, the natural frequencies are obtained in unit of Hertz (Hz) from Equation 3.51. In order to compare the results of present study with the results of study in literature, the values of natural frequencies are normalized with following equation.

$$\Omega = \omega a^2 \left(\frac{\rho}{D_0} \right)^{1/2} \tag{3.52}$$

where ω and Ω are angular natural frequency (also referred to by the terms radial frequency, circular frequency) and nondimensionalised natural frequency, respectively. The reference bending rigidity D_0 is:

$$D_0 = \frac{1}{12} \frac{E_2 t^3}{1 - \upsilon_{12}\upsilon_{21}} \tag{3.53}$$

CHAPTER 4

OPTIMIZATION

4.1. General Information

Optimization is commonly used, from engineering design to financial markets, from our daily activity to planning our holidays, and computer sciences to industrial applications. People always would like to choose the optimum and tend to maximize or minimize something by using the constraints. In fact, we are continuously searching for the optimal solutions to every problem that we face, however we are not necessarily able to find such solutions (Xin-SheYang, 2010).

Optimization is a mathematical procedure for determining optimal allocation of limited resources. Generally, an optimization problem has an objective function (fitness function) that determines efficiency of the design. Objective function can be classified into two groups: single objective and multi-objective. An optimization process is usually performed within some limits that determine the solution space. These limits are defined as constraint. Lastly, an optimization problem has design variables, which are parameters that are changed during the design process. Design variables can be dispersed (continuous) or discrete (limited continuous). A special case of discrete variables are integer variables.

Generally, even though the objective function is minimized, for the cases of the engineering problems, it is maximized. For instance, stiffness and buckling load factor are maximized for laminated composite material. Maximizing or minimizing some function is relative to some set, often representing a range of choices available in a certain situation. The function allows comparison of the different choices for determining which might be “best”. Engineers have to take many decisions at several stages. The ultimate goal of all such decisions is either to minimize the effort required or to maximize the desired benefit. The process of adjusting the inputs of a device, mathematical process, or experiment is to find the minimum or maximum output. It can be seen from Figure 4.1 that if a point x* corresponds to the minimum value of function $f(x)$, the same point also corresponds to the maximum value of the negative of the

function, $-f(x)$. Consequently, without loss of generality, optimization can be taken to mean minimization because the maximum of a function can be found by searching for the minimum of the negative of the same function (Rao, 2009).

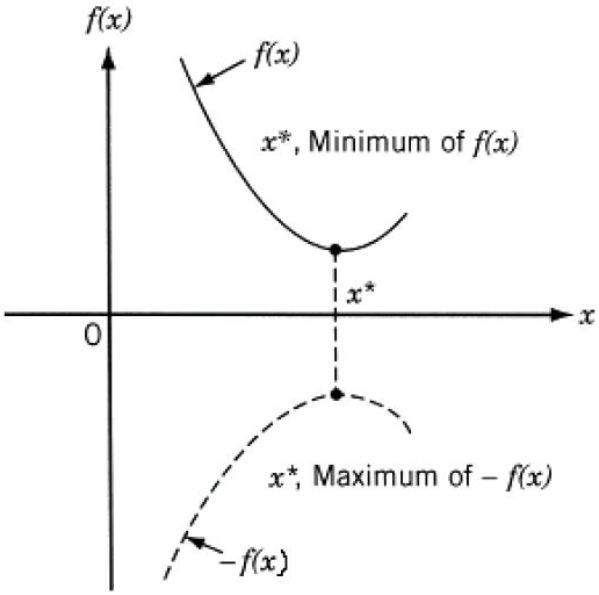

Figure 4.1. Minimum and maximum of objective function ($f(x)$)
(Source: Rao 2009)

An optimization algorithm is a procedure which is executed iteratively by comparing various solutions till an optimum or a satisfactory solution is found. With the advent of computers, optimization has become a part of computer aided design activities. There are two distinct types of optimization algorithms widely used today:
(a) deterministic algorithms, (b) stochastic algorithms. These terms can be defined as follows:

(a) Deterministic Algorithms: They use specific rules for moving one solution to other. These algorithms are in use to suite some times and have been successfully applied for many engineering design problems.

(b) Stochastic Algorithms: The stochastic algorithms are in nature with probabilistic translation rules. These are very popular due to certain properties which deterministic algorithms do not have.

Composite design problems generally are very complicated and it is not possible to solve by the traditional optimization techniques. In this case, the modern optimization methods have come up as powerful and popular methods for solving complex engineering optimization problems. Genetic Algorithms (GA), Generalized Pattern Search Algorithm (GPSA), Particle Swarm Optimization (PSO), Ant Colony Optimization (ACO) and Simulated Annealing (SA) can be counted as the stochastic optimization methods. In composite laminate design problems, derivative calculations or their approximations are impossible to obtain or is often costly. Therefore, stochastic search methods have the advantage of requiring no gradient information of the objective functions and the constraints. A deterministic algorithm, where a monotonically decreasing value of an objective function is iteratively created, may stuck into any local optimum point rather than globally optimum one in relation to the starting point. Thus, the choice of initial design is an important factor in its success. In this respect, the common approach might be to employ the algorithm several times starting from different configurations with the aim that one of the first positions be sufficiently close to the globally optimum configuration, and then to find out the lowest value as the globally optimum solution. If the starting point is outside the feasible region, the algorithm may converge to a local optimum within the infeasible domain which may be regarded as another disadvantage.

4.2. Definition of Optimization Problem

The standard formulation of optimization problem can be stated as follows:

$$\text{Find } X = \begin{Bmatrix} x_1 \\ x_2 \\ \vdots \\ x_n \end{Bmatrix} \text{ which minimizes } f(x) \tag{4.1}$$

subjected to the constraints

$$g_i(X) \leq 0, \qquad i = 1, 2.....m$$

$$h_i(X) = 0, \qquad i = 1, 2..... \text{p}$$

where $f(\text{X})$ is an objective function, $g(\text{X})$ and $h(\text{X})$ are inequality and equality constrains, respectively. The number of variables n and the number of constraints m and/or p are not necessary to be related in any way. The optimization problem stated in Equation 4.1 is called a constrained optimization problem. There are not any constraints in some optimization problems which are called unconstrained optimization problems (Rao, 2009).

The formulation of an optimization problem begins with identifying the underlying design variables, which are primarily varied during the optimization process. A design problem usually involves many design parameters, of which some are highly sensitive to the proper working of the design. These parameters are called design variables in the parlance of optimization procedures. Other (not so important) design parameters usually remain fixed or vary in relation to the design variables. The first thumb rule of the formulation of an optimization problem is to choose as few design variables as possible. The outcome of that optimization procedure may indicate whether to include more design variables in a revised formulation or to replace some previously considered design variables with new design variables.

The constraints represent some functional relationships among the design variables and other design parameters satisfying certain physical phenomenon and certain resource limitations. The nature and number of constraints to be included in the formulation depend on the user. Constraints may have exact mathematical expressions or not.

4.3. Genetic Algorithm (GA)

The Genetic Algorithm (GA) is a stochastic optimization and search technique which allows obtaining alternative solutions for some of the complex engineering problems such as increasing composite strength, developing dimensionally stable and light weight structures, etc. GA method utilizes the principles of genetics and natural selection. This method is simple to understand and uses three simple operators:

selection, crossover and mutation. Genetic Algorithm always considers a population of solutions instead of a single solution at each iteration. It has some advantages in parallelism and robustness of genetic algorithms. It also improves the chance of finding the global optimum point and helps to avoid local stationary point. However, GA is not guaranteed to find the global optimum solution to a problem. GA has been applied to the design of a variety of composite structures ranging from simple rectangular plates to complex geometries. Genetic algorithms have been widely used in laminate design optimization problems because of the fact that they are suitable for integer programming and able to find global optima.

4.3.1. Crossover

Crossover, one of the basic genetic algorithm operators, is responsible for the exchange of genetic information among the individuals of the population. A few types of crossover have been used in the composite materials, such as: one-point, two-point and uniform crossover (Figure 4.2). The effective of each type of crossover may depend on the optimization problem and also the stage of the search (Lopez, et al. 2009).

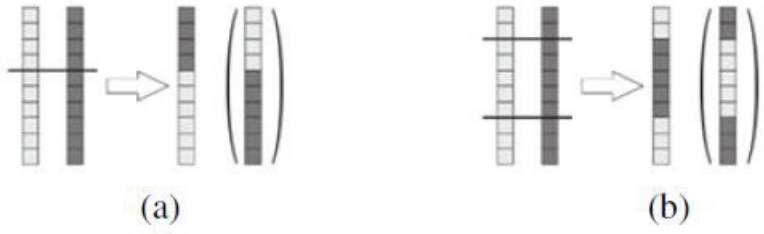

Figure 4.2. Types of crossover (a) One-point crossover (b) Two-point crossover (Source: Weise 2009)

4.3.2. Mutation

The other basic genetic algorithm operator, the mutation, changes randomly the value of the genes of the individuals and unexplored regions of the design space can be

found for valuable solution. Mutation is applied by generating a random number between 0 and 1 (Gurdal, et al. 1999). In Figure 4.3, three types of mutation are shown.

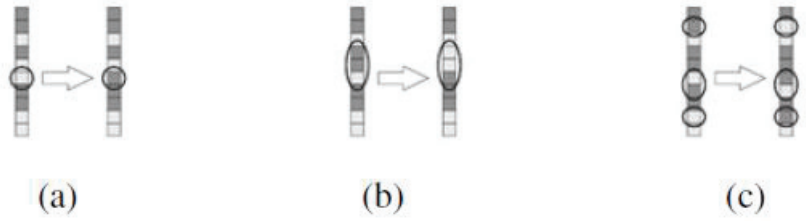

Figure 4.3. Value-altering mutation of strings (a) Single-gene mutation (b) Multi-gene mutation (c) Multi-gene mutation (Source: Weise, 2009)

4.3.3. Selection

Selection is the process of choosing two parents from the current population for crossing. After deciding on an encoding, the next step is to determine how to perform selection i.e., how to choose individuals in the population which will create offspring for the next generation and how many offspring each will create. The aim of selection is to highlight fitter individuals in the population in hopes that their off springs have higher fitness.

4.4. Generalized Pattern Search Algorithm (GPSA)

Generalized Pattern Search Algorithm has been defined for derivative-free unconstrained optimization of functions by Torczon (1997) and later extended to take nonlinear constrained optimization problems into account. GPSA is a direct search method which finds a sequence of points that approach the optimal point. Each iteration is divided into two phases: the search phase and the poll phase. In the search phase, the objective function is evaluated at a finite number of points on a mesh. The main task of the search phase is to find a new point that has a lower objective function value than the best current solution which is called the incumbent. In the poll phase, the objective function is evaluated at the neighboring mesh points, so as to see whether a lower

objective function value can be obtained (Nicosia, 2008). GPSA has some collection of vectors that form the pattern and has two commonly used positive basis sets; the maximal basis with 2N vectors and the minimal basis with N+1 vector.

In order to clarify the algorithm, a laminated composite plate optimization problem including two independent variables θ_1 and θ_2 in the objective function has been considered. In this case, pattern consists of the vectors $v_1[1\ \ 0], v_2[0\ \ 1], v_3[-1\ \ 0], v_4[0\ \ -1]$ for the positive basis *2N* or $v_1[1\ \ 0], v_2[0\ \ 1], v_3[-1\ \ 0], v_4[0\ \ -1]$ for the positive basis *N+1*. The pattern search begins at a provided initial point vector θ_0. In this example problem, $\theta_0 = [10\ \ 50]$, the mesh size $\Delta^m = 5$ and positive basis *2N* are taken into account. At the first iteration, the following mesh points can be calculated as

$$[1\ \ 0]x5+[10\ \ 50]=[15\ \ 50]$$
$$[0\ \ 1]x5+[10\ \ 50]=[10\ \ 55]$$
$$[-1\ \ 0]x5+[10\ \ 50]=[5\ \ 50]$$
$$[0\ \ -1]x5+[10\ \ 50]=[10\ \ 45]$$

and the algorithm computes the objective function at these mesh points before polls. If the algorithm finds an objective function value which is smaller than the value at $\theta_0 = [10\ \ 50]$, the poll at corresponding iteration is called as "successful". Supposing the vector [10 55] satisfies the condition, the algorithm sets the next point in the sequence equal to $\theta_0 = [10\ \ 55]$. After obtaining a successful poll, the algorithm multiplies the current mesh size by expansion factor. For example, if the expansion factor is taken as 2, the mesh size for the second iteration becomes 5x2=10 and the mesh at the second iteration is to be

$$[1\ \ 0]x10+[10\ \ 55]=[20\ \ 55]$$
$$[0\ \ 1]x10+[10\ \ 55]=[10\ \ 65]$$
$$[-1\ \ 0]x10+[10\ \ 55]=[0\ \ 50]$$
$$[0\ \ -1]x10+[10\ \ 55]=[10\ \ 45]$$

Now, suppose that produce smaller objective function value than the value at $\theta_0 = [10\ \ 55]$. This procedure repeats until none of the mesh points has a smaller objective function value than the value at last (say n) successful poll iteration. This poll

is called as “unsuccessful” in the corresponding iteration. In this case, the algorithm does not change the current point at the next iteration as $\theta_{n+1} = \theta_n$. In such a case, the algorithm multiplies the current mesh size by given *contraction factor* and the algorithm then polls with a smaller mesh size. The algorithm stops when any of the stopping criteria conditions satisfied.

4.5. Matlab Optimization Toolbox

MATLAB Global Optimization Toolbox provides methods that search for global solutions to problems that include multiple maxima or minima. It contains global search, multistart, pattern search, genetic algorithm, and simulated annealing solvers. These solvers to solve optimization problems where the objective or constraint function is continuous, discontinuous, stochastic, does not possess derivatives, or includes simulations or black-box functions with undefined values for some parameter settings. Figure 4.4 shows genetic algorithm solver menu of MATLAB.

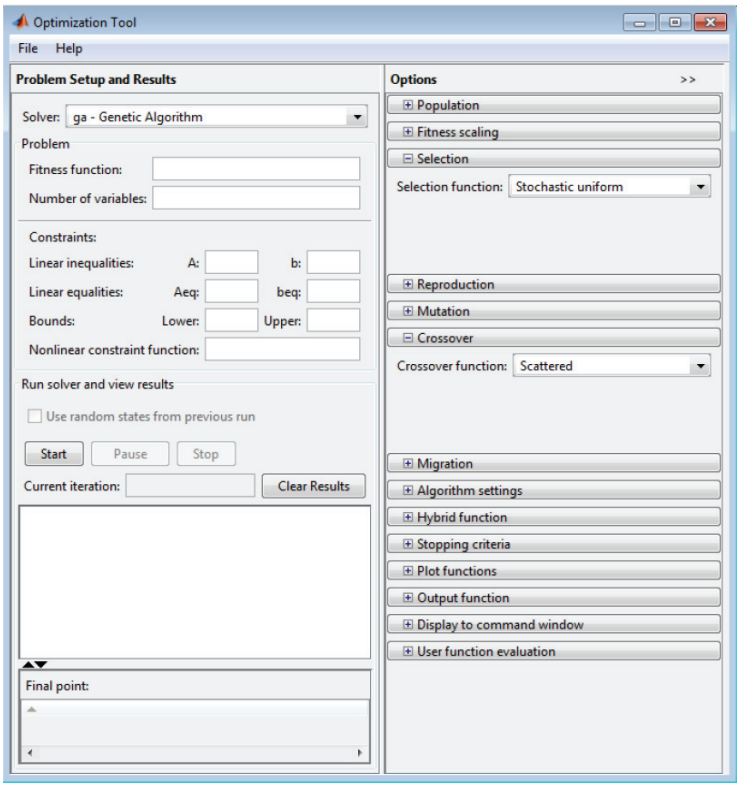

Figure 4.4. Matlab optimization toolbox ga solver user interface

Genetic Algorithm Toolbox of MATLAB consists of two main parts. The first part is problem definition (fitness function and number of variables) and constraints (linear inequalities, linear equalities, bounds and nonlinear constraint function). The second is options (population, fitness scaling, selection, reproduction, mutation, crossover, migration, algorithm settings, hybrid function, stopping criteria, plot functions, output function, display to command window and user function evaluation). Population determines the size of population at each of iteration. In this study, the genetic algorithm options parameters shown in Table 4.1are used.

Table 4.1. Genetic Algorithm parameters for single objective function

Population type	Double vector
Population size	40
Creation function	Use constraint dependent
Initial range	[-90:90]
Scaling function	Rank
Selection function	Roulette
Elite count	2
Mutation function	Use constraint dependent
Crossover fraction	Scattered
Migration direction	Both Fraction=0.2, Interval_20
Initial penalty	10
Penalty factor	100
Hybrid function	Patternsearch
Stopping criteria	Generations = 1000 Stall generations =1000 Function tolerance = 10^-6

4.5.1. Hybrid Algorithm Solver

The optimization procedure which describes how GPSA works and interacts with GA in the hybrid algorithm is given in Figure 4.5 and explained step by step as follows (Deveci and Artem, 2017):

Step 1. GA runs until either the maximum number of iterations is reached or there is no improvement in the fitness value.

Step 2. When GA terminates, the reached optimal solution is used as an initial point for GPSA to search.

Step 3. GPSA starts its search with an initial solution x_0 and an initial mesh size Δ_0^m.

Step 4. If the search phase satisfies a solution with a lower objective function value than the best current solution, the algorithm stops.

Step 5. If termination criteria not satisfied, the algorithm goes to the poll phase and generates a set of neighboring mesh points X_i^m by multiplying the current mesh size by each pattern vector $\{d_i\}$. The fixed-direction pattern vectors are used to determine the points to search at each iteration and defined by the independent variables in the objective function; commonly the maximal basis with 2N vectors consisting of N positive and N negative vectors, and the minimal basis with N + 1 vectors.

Step 6. In the polling step at *k*th iteration, GPSA polls all the mesh points by computing their objective function values $f\left(X_i^m\right)$ in order to find an improved point.

Step 7. If the poll is successful, which means an improved point is found, the current mesh size is multiplied as $\Delta_{i+1}^m = 2\Delta_i^m$, and the current point is updated by the new mesh size for the next iteration k + 1. If the polling fails to find an improved point, the mesh size is reduced by $\Delta_{i+1}^m = 0.5\Delta_i^m$, and this current point is used for the next iteration. This process continues through many iteration until global optimum is reached.

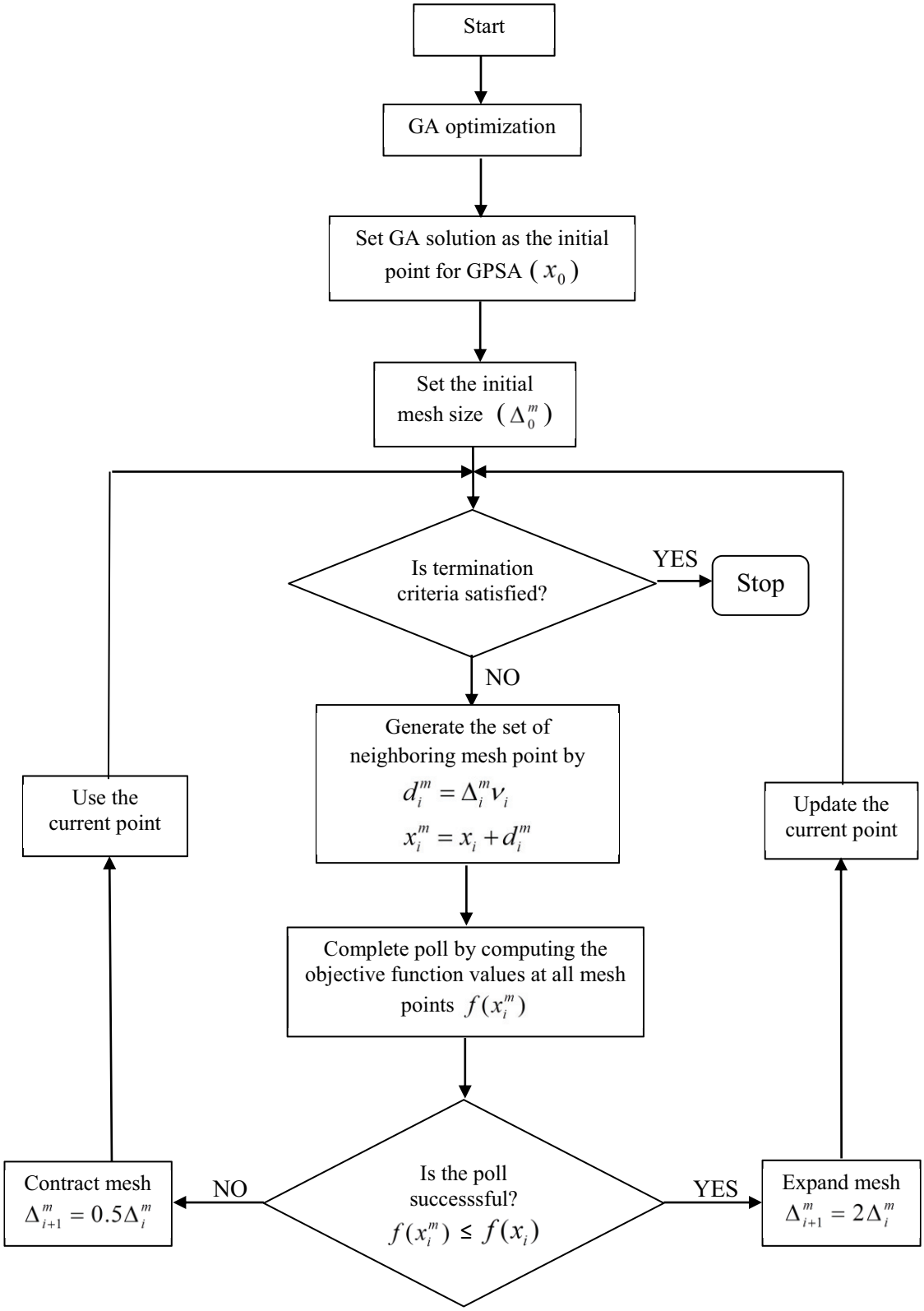

Figure 4.5. Flowchart of the hybrid algorithm optimization
(Source: Deveci and Artem, 2017)

CHAPTER 5

FINITE ELEMENT METHOD

5.1. Introduction

The finite element metod (FEM) is a numerical method widely used to obtain approximate solution of boundary value problems in engineering. Analytical solutions are usually not obtainable for the physical systems having complicated geometries, loadings, and material properties. Hence, the numerical methods such as finite element are required. The finite element method is powerful anaysis technique used to overcome challenging structural problems. The finite element method (FEM) has developed into a key indispensable technology in the modeling and simulation of advanced engineering systems in various fields like housing, transportation, communications, and so on. In building an advanced engineering system, engineers and designers go through a sophisticated process of modeling, simulation, visualization, analysis, design, prototyping, testing, and lastly, fabrication. More often than not, much work is involved before the fabrication of the final product or system. This is to ensure the workability of the finished product, as well as for cost effectiveness in the manufacturing process. The finite element method has first used to solve problems of stress analysis, and has since been applied to many other problems like heat transfer, fluid flow, mass transport, electromagnetic potential, and many other. The knowledge of deformations, stress-strain patterns, temperature flow or fluid flow in any system subjected to an external loading or pressure can be obtained at the results of the analysis. In this method, analyze models of complex shapes defining a continuum is discretized into simple geometric shapes called finite elements. A displacement function is associated with each finite element. Every interconnected element is linked to each other at the points called nodes as shown Figure 5.1. The degrees of freedom, which are the number of independent movements possible, are represented by the nodes.

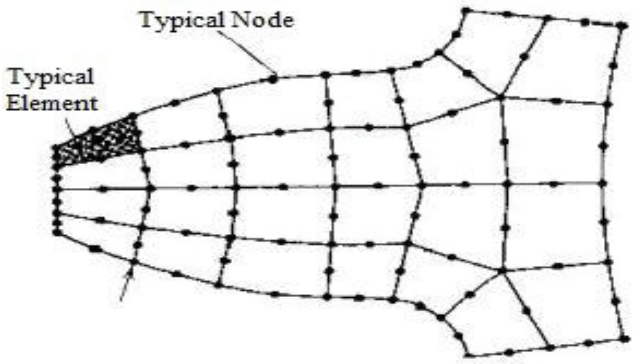

Figure 5.1. Typical finite element mesh

The total equilibrium equations describing the behavior of each node gives a series of algebraic equations expressed in matrix notation. In finite element, instead of seeking the solution for the entire domain in one step, the equations are formulated for each finite element and then combine them to achieve whole domain. Briefly, the solution of the problem depends on determining the displecements at each node and stresses within the each element

.

5.2. General Steps of Finite Element Method

The behavior of a physical phenomenon in a system depends upon the geometry or domain of the system, the property of the material or medium, and the boundary, initial, and loading conditions. For an engineering system, the geometry or domain can be very complex. Furthermore, the boundary and initial conditions can also be very complicated. It is therefore, in general, very difficult to solve the governing differential equation via analytical means. In practice, most of the problems are solved using numerical methods. Among these, the methods of domain discretization championed by the FEM are the most popular due to their reliability, practicality, versatility, and robustness. The solution of a continuum problem by the finite element method always follows an orderly step by step process. Procedures can be stated as follows:

1. Discretize the continuum and select the element types: the first step involves dividing a solution region into finite elements and choosing the most suitable element type to model defining closely the actual physical behavior of the body. Many different types of elements used in FEM is available. These elements are improved independently

and vary from one finite element (FE) software to another. In general, there are three groups of element which are one-dimensional (1D), two-dimensional (2D), and three-dimensional (3D) elements. These elements that are commonly employed in practice are shown in Figures 5.2, 5.3 and 5.4. The finite element mesh is typically created by a preprocessor program.

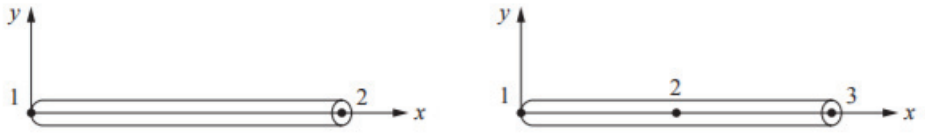

Figure 5.2. Simple one-dimensional line element
(Source: Logan, 2011)

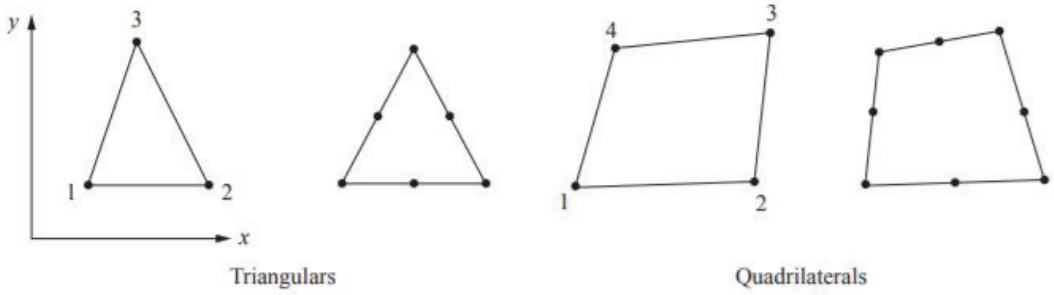

Figure 5.3. Simple two-dimensional elements with corner nodes and intermediate nodes
(Source: Logan, 2011)

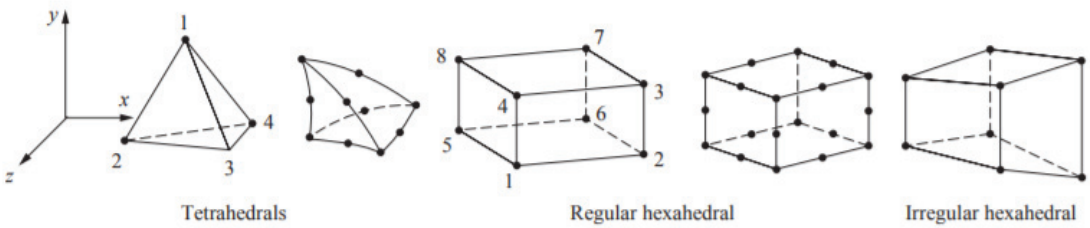

Figure 5.4. Simple three-dimensional elements with corner nodes and intermediate nodes (Source: Logan, 2011)

2. Select interpolation functions: the second step involves choosing a displacement function within each element. In general, polynomials are selected as interpolation functions. The degree of the polynomial depends on the number of nodes assigned to the element.

3. Find the element properties: the third step involves establishing the matrix equation for the finite element, which is related to the nodal values of the unknown function to other parameters. The variational approach and the Galerkin method are the most convenient for this task.

4. Assemble the element equations: all the element equations is assembled to find the global equation system in whole solution region. In other words, local element equations for all elements used for discretization are combined. Element connectivities are used for the assembly process. Before solution step, boundary conditions should be defined.

5. Solve the global equation system: direct and iterative methods can be used for the finite element global equation sytem. The nodal values of the searching function are produced as a result of the solution.

6. Compute additional results: the main aim is to interpret the results for use in desing process. The results interested in values of principal stresses, heat fluxes, strains, etc can be obtained and computer programs helps the user by displaying them in graphical form.

5.3. Finite Element Modeling Using ANSYS

ANSYS is one of the most comman finite element modeling (FEM) software used to predict the physical behaviour of systems and structures and can be applied to a large number of engineering applications due to its trustworthiness in design and analysis. It helps to predict the responses of various products, parts, subassemblies and assemblies by simulating the real life cases as par to the experimental results. Modelling and simulation step helps to reduce time of prototyping and moderates the physical verification expenses. It also increases the innovation at a faster rate. The optimization step in FEM tool adds a new paradigm to achieve the designer quest. ANSYS is now being used in a number of different engineering fields such as power generation,

transportation, medical components, electronic devices, and household appliances for its easy applicability.

The first ANSYS concept was discussed in a public forum during 1976. The designing was improved slowly from 2D-3D modeling. Initially, the modeling was confined to beam to shell and then it is extended to volume elements. In addition to that, graphics were introduced for better modeling and prediction. It is well known that, the FEM was initially involved to discretize the structure into nodes and joining them by specific rule elements are obtained and the respective responses are calculated. Today ANSYS can be used many fields such as fatigue analysis, nuclear power plant, medical applications, and to find the eigenvalues of magnetic field, etc. ANSYS is also very useful in electro-thermal analysis of switching elements of a super conductor, ion projection lithography, detuning of an HF oscillator by the mechanical vibration of an acoustic sounder. It is used to analyze the vehicle simulation and in aerospace industries as well.

Based on the above discussion on the capability of ANSYS, in this thesis, finite element analysis method have been applied to the numerical study of laminated composite plate and all analysis have been done by using ANSYS code, and by the Graphical User Interface (GUI). The three dimensional model have been built and the shell 8 node 281 have been used. Shell 281 is well-suited for analying thin to moderately-thick shell structures. The element has eight node with six degree of freedom at each node.

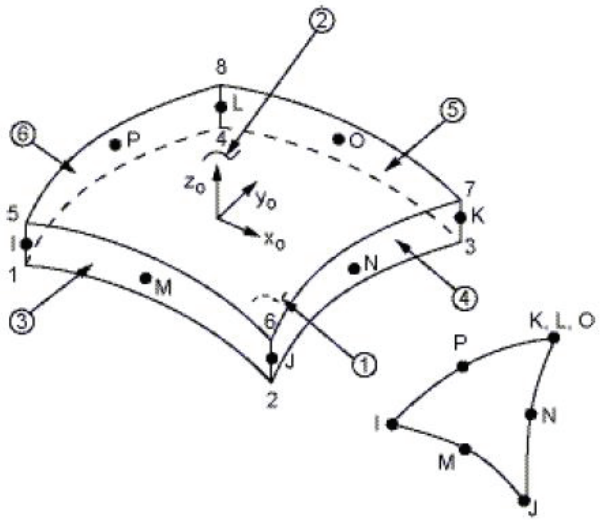

Figure 5.5. 8 node 281 shell element

5.4. Modal Analysis in ANSYS

Modal analysis is, along with linear static analysis, one of the most common types of finite element analysis. The purpose of a modal analysis is to find the mode shapes and natural frequencies at which the structure will amplify the effect of a load in design stages. All structures have the tendency to vibrate at certain frequencies called natural or resonant frequencies and each natural frequency is associated with a certain shape, called mode shape. Figure 5.6 shows representatively the natural frequencies and mode shapes of beam. The natural frequencies and mode shapes are important parameters in the design of a structure for dynamic loading conditions. It also is a starting point for another dynamic analysis, such as a transient dynamic analysis, a harmonic response analysis, or a spectrum analysis.

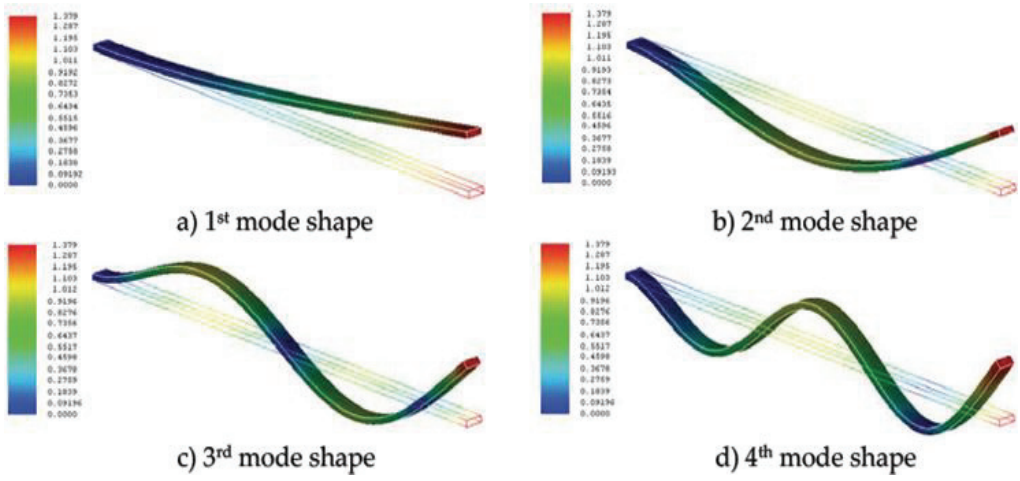

Figure 5.6. Mode shapes of the cantilever beam model

In the modal analysis, the dynamic equations of motion of a structure can be derived by using either Lagrange equations or Hamilton's principle. By using finite element method, the final equilibrium equation of motion can be written as

$$[M]\{\ddot{\delta}\}+[C]\{\dot{\delta}\}+[K]\{\delta\}=\{F(t)\} \tag{5.1}$$

where $[K]$, $[M]$ and $[C]$ are stiffness matrix, mass matrix and damping matrix, respectively. $F(t)$ is an externally applied force. Modal analysis is an analysis of the

vibration characteristics of the structure under free vibration, which means that no time varying external forces act on the system and the damping is generally negligible, then it becomes as follows:

$$[M]\{\ddot{\delta}\}+[K]\{\delta\}=0 \tag{5.2}$$

The free vibration of the elastic body can be transformed into a combination of a series of simple vibrations, which can be used to obtain the natural frequencies of the free vibration and the modes of each order:

$$\{\delta\}=\{\delta_0\}\sin(\omega x+\phi) \tag{5.3}$$

Then substitution of Equation 5.3 into Equation 5.2:

$$\left([K]-\omega^2[M]\right)\{\delta_0\}=0 \tag{5.4}$$

For the free vibration, the amplitude of each point in the structure will not be completely zero, so the value of the matrix determinant in the above formula must be zero, so the free vibration frequency equation can be described as follow:

$$\left|[K]-\omega^2[M]\right|=0 \tag{5.5}$$

These values are for all n matrix, where n is the number of node degrees of freedom, so the formula is about n times real coefficient equation of freedom. From the solution of N real root ω_i^2 $(i=1,2,3,...,\mathrm{n})$, the characteristic value is obtained according to the ascending order as follows:

$$\omega_1^2 \le \omega_2^2 \le \omega_3^2 ... \le \omega_n^2 \tag{5.6}$$

The corresponding vector $\{\delta_0^{\,i}\}(i=1,2,3...,n)$ can be solved by the return equation of any ω_i^2 generation.

The solution procedure for a modal analysis in ANSYS consists of four main steps:

- Build the model.
- Apply boundary conditions and obtain the solution.
- Expand the modes.
- Review the result

Some inputs are required to do modal analysis in FEA software. These are called as EIGL card, which is a way to enter the parameter for modal analysis. EIGL card involves as following information. Modal anaysis options in ANSYS are shown in Figure 5.7.

1- The initial frequency (V_1): suitable initial frequency where the structure will start to vibrate is written.
2- The last frequency (V_2): suitable last frequency where the structure will stop to vibrate is written.
3- The number of modes (N): the number of modes of interest is written in the analysis.

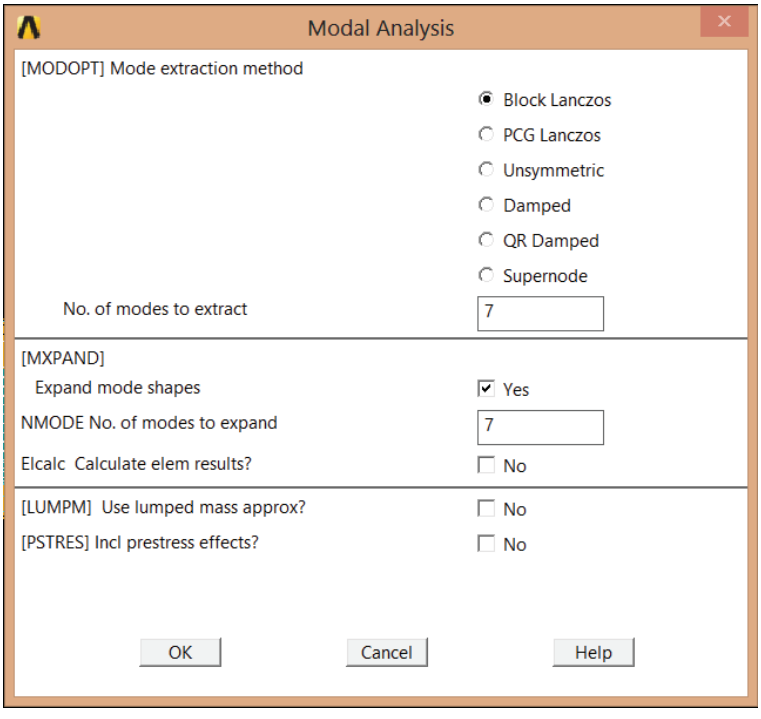

Figure 5.7. Modal analysis options in ANSYS

CHAPTER 6

RESULTS AND DISCUSSIONS

6.1. Problem Definition

The objective of this study is to investigate the optimum stacking sequence design of laminated composite plates for free vibration behavior by using the hybrid algorithm combining genetic algorithm and generalized pattern search algorihm (GA/GPSA) and the finite element method (FEM).

The composite plate with width of a and length of b is subjected to the combination of three different boundary conditions, free (F), simply supported (S) and clamped (C). These conditions are assumed along the plate edges 1, 2, 3, 4 shown in Figure 6.1. In application of boundary conditions, the notation SFCF denotes the composite plates with edges 1, 2, 3, 4 having the simply supported, free, clamped and free boundary conditions, respectively. The material of composite plate is graphite/epoxy. The laminate is symmetric and each of the lamina has the same thickness.

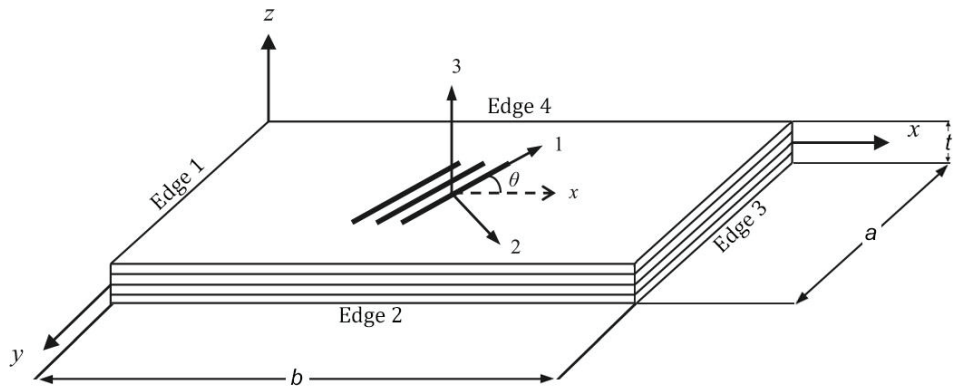

Figure 6.1. Edge numbering and coordinate system of the laminated composite plate

The width of plate is a = 0.20m and a total ply thickness is t = 0.002m. The lenght of plate b changes with respect to aspect ratios considered. Non-dimensionalized

fundamental frequencies have been computed in aspect ratios; *k =1, 2, 3, 4, 5* and in combination of boundary conditions for each number of ply; *n = 4, 8, 16*. Effect of material orthotropy degree on fundamental frequency of laminated composite plate has also been examined.

The elastic properties of the layers have been taken from previous studies (Narita, 2003) and given in Table 6.1.

Table 6.1. The elastic properties of graphite/epoxy layers
(Source: Narita, 2003)

Material	Longitudinal modulus E_1(GPa)	Transverse modulus E_2 (GPa)	Shear modulus G_{12} (GPa)	Poisson's ratio v_{12}	Density ρ (kg/m^3)
Graphite/epoxy	138	8.96	7.1	0.3	1600

During design process, fiber orientation angles of the plate have been considered as design variables and been taken as continuous ($-90 \leq \theta \leq 90$). Stacking sequence of N-layered composite plate can be given representatively as

$$[\pm\theta_1/\pm\theta_2/\pm\theta_3/\pm\theta_4/\pm\theta_5/\pm\theta_6/\pm\theta_7/\pm\theta_8/\ \ldots\ldots\ldots\ldots/\pm\theta_{n-1}/\pm\theta_n]_s$$

The mathematical schema of the optimization problem for this study can be stated as follow:

Find : $\theta = (\theta_1, \theta_2, ..., \theta_k)$
Maximize : $\Omega = \Omega(\theta_1, \theta_2, ..., \theta_k)$
Subject to : $-90^\circ \leq \theta_k \leq 90^\circ$

Free vibration equation where The Rayleigh-Ritz method is utilized for finding the approximate solution under different boundary conditions has been used as an objective function in optimization. The objective function for each design parameter has been calculated using the MATLAB *Symbolic Math Toolbox* and the algorithm is given in Appendix A. Fundamental frequency of laminated composite has been maximized by

using hybrid algorithm (GA/GPSA). Finally, modal analysis has been performed in order to verify optimization results in ANSYS. Fiber orientations obtained from optimization process have been taken as input parameters for FEM solution. APDL code of the finite element method is given in Appendix B.

6.2. The Verification of Algorithms and Modeling

In this study, the laminated composite plates have been analyzed to find the optimum stacking sequence by using the hybrid optimization algorithm for different number of ply, plate aspect ratios, boundary condition and degree of material orthotropy. The algorithms for vibration behavior of composite plate have been written in MATLAB. The reliability of algorithms computing the natural frequency of laminated composite plate (Equation 3.51) has been tested with the study in literature (Narita, 2003). In order to demonstrate efficiency and reliability of GA,

- 30 independent iterations have been carried out for each case,
- GA Toolbox options have been adjusted as shown in Table 4.1,
- Genetic Algorithm combined with *Generalized Pattern Search Algorithm* (GPSA) has been used in order to obtain a hybrid algorithm solution.

Narita (2003) presented the layer-wise optimization approach to maximize the first natural frequency of laminated composite plate and utilized Rayleigh-Ritz equation to find approximate solutions with different boundary condition. The optimum results have been obtained for symmetric 8-layered composite plates with various boundary conditions and aspect ratios (a/b = 1 and a/b = 2). First, the natural frequency parameters in the optimum stacking sequences given by Narita (2003) are compared with the finite element method. The plate has been divided into quadrilateral elements. While the geometry and element type of composite plate are generated in two dimensional spaces, thickness must also be taken into consideration. Therefore, two-dimensional mesh is now converted to three dimensional mesh by means of shell element. Three-dimensional mesh is typically shown in Figure 6.2.

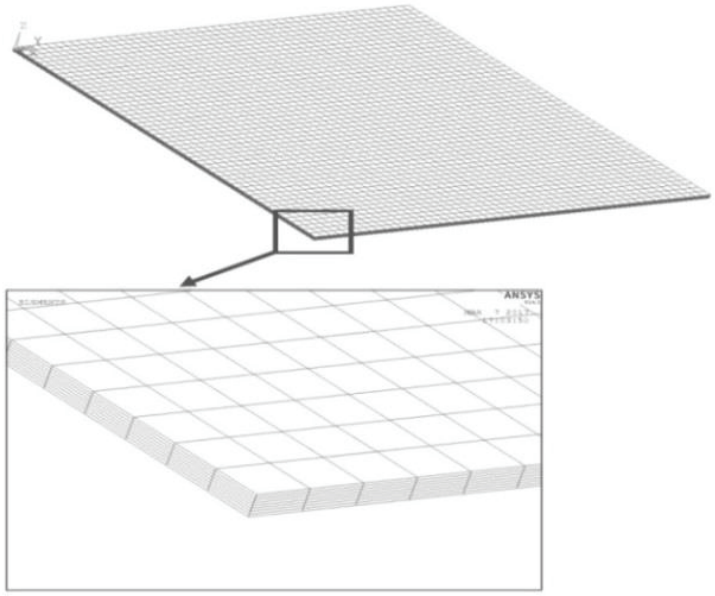

Figure 6.2. The finite element model of symmetric 8-layered composite plate

In addition, accuracy of the solution that can be obtained from FEM model is directly related with mesh used. FEM also requires certain computational time to solve the problems. Although dividing the structure with the finer mesh elements results in the more accurate solution, it takes a large amount of computer memory and long run times. For these reasons, mesh convergence test has been conducted to determine the optimum size of the elements in all aspect ratio values and in SSCF boundary condition. As shown in Figure 6.3, mesh size 50x50 that is sufficient for all aspect ratios has been used for analysis. The optimization was carried out on a single processor computer with 2.4 GHz Intel Core İ7 including 4GB memory, and the total computational time needed was about 15-20 sec. on a personal computer.

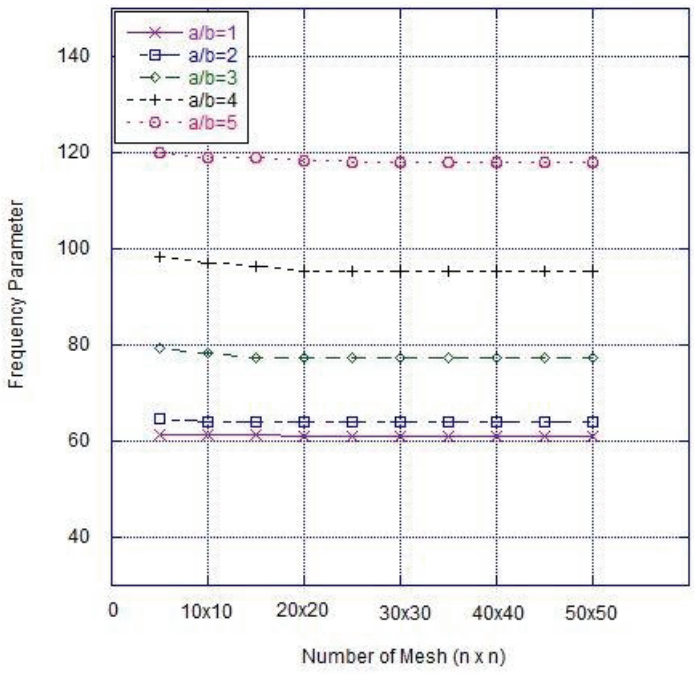

Figure 6.3. Mesh convergence for all aspect ratios

Then, the optimal stacking sequences in various combinations of boundary conditions for the first natural frequency of composite plate are investigated by using Genetic Algorithm (GA) and Generalized Pattern Search Algorithm (GPSA) constituting the hybrid solution, coupled with a finite element code to obtain the structural response. The fiber angles of each ply in the composite plate are taken with $\Delta\theta = 1^\circ$ increment between $-90^\circ \leq \theta_k \leq 90^\circ$. Verification algorithm and finite element modeling for symmetric 8-layered square plate with various boundary conditions are given in Tables 6.2 and 6.3. The results are compared with those of given by Narita. It can be observed that the hybrid algorithm predicts successfully the optimal stacking sequences that give the maximum natural frequency.

Table 6.2. Verification of objective function algorithm and finite element modeling for symmetric 8-layered square plate with various boundary conditions (a/b = 1)

BC's	Optimal Stacking (Narita, 2003)	Ω_{opt} (Narita, 2003)	Ω_{opt} FEM	Optimal Stacking (Present Study)	Ω_{opt} (Present Study)	Ω_{opt} FEM (Present Study)
SSFF	$[-45/45/-45/45]_s$	11.28	11.10	$[-45/45/-45/45]_s$	11.92	11.10
CFFF	$[0/0/0/0]_s$	13.79	13.78	$[0/0/0/0]_s$	13.79	13.78
SCFF	$[75/-50/65/65]_s$	16.28	16.20	$[54/-54/-54/-54]_s$	17.22	16.64
CCFF	$[65/-35/40/40]_s$	18.80	18.70	$[45/-45/-45/-45]_s$	19.16	18.79
SFSF	$[0/0/0/0]_s$	38.69	38.65	$[0/0/0/0]_s$	38.71	38.65
SFCF	$[0/0/0/0]_s$	60.47	60.30	$[0/0/0/0]_s$	60.49	60.30
SSSF	$[0/0/0/0]_s$	39.84	39.77	$[0/0/0/0]_s$	39.89	39.77
SCSF	$[0/0/0/0]_s$	40.28	40.21	$[0/0/0/0]_s$	40.62	40.21
SSCF	$[-5/0/-5/-5]_s$	61.49	61.27	$[0/0/0/0]_s$	61.38	61.15
SCCF	$[-5/-5/0/0]_s$	61.88	61.66	$[0/0/0/0]_s$	61.91	61.45
CFCF	$[0/0/0/0]_s$	87.77	87.34	$[0/0/0/0]_s$	87.80	87.34
CSCF	$[0/0/0/0]_s$	88.41	87.96	$[0/0/0/0]_s$	88.46	87.96
CCCF	$[0/0/0/0]_s$	88.63	88.18	$[0/0/0/0]_s$	88.85	88.18
SSSS	$[45/-45/-45/-45]_s$	56.32	55.48	$[-45/45/45/45]_S$	56.49	55.48
SSSC	$[90/75/-60/-60]_s$	65.27	64.97	$[59/-59/-59/-59]_S$	67.06	66.10
SSCC	$[0/45/-45/-45]_s$	68.72	68.32	$[45/-45/-45/-45]_s$	73.45	72.52
SCSC	$[90/90/90/90]_s$	90.89	90.37	$[90/90/90/90]_s$	90.89	90.37
CCCS	$[0/0/0/0]_s$	91.99	91.48	$[0/0/0/0]_s$	92.07	91.48
CCCC	$[0/90/0/90]_s$	93.67	93.31	$[90/90/90/90]_S$	93.69	93.16

It can be seen from in Table 6.2, frequency values for symmetric 8-layered square composite plate (a/b=1) are very close to compared study (Narita, 2003). Results show that natural frequency of the composite plate increases as the boundary conditions of plate is clamped. The maximum natural frequency occurs at CCCC boundary condition. On the contrary, the minimal value of natural frequency is obtained for the plate having SSFF boundary condition. Since clamped boundary condition have less degree of freedom, it is more effective to stiffen the structure.

Table 6.3 Verification of objective function algorithm and finite element modeling for symmetric 8-layered plate with various boundary conditions (a/b = 2)

BC's	Optimal Stacking (Narita, 2003)	Ω_{opt} (Narita, 2003)	Ω_{opt} FEM	Optimal Stacking (Present Study)	Ω_{opt} (Present Study)	Ω_{opt}FEM (Present Study)
SSFF	$[-35/45/-45/45]_s$	21.89	21.45	$[-45/45/45/-45]_s$	22.55	21.72
CFFF	$[0/0/0/0]_s$	13.79	13.78	$[0/0/0/0]_s$	13.79	13.78
SCFF	$[85/85/85/85]_s$	57.06	56.92	$[90/90/90/90]_s$	56.76	56.35
CCFF	$[85/85/85/85]_s$	57.71	56.57	$[90/90/90/90]_s$	57.72	56.76
SFSF	$[0/0/0/0]_s$	38.66	38.62	$[0/0/0/0]_s$	38.71	38.62
SFCF	$[0/0/0/0]_s$	60.44	60.27	$[0/0/0/0]_s$	60.49	60.27
SSSF	$[0/-30/40/35]_s$	45.26	44.81	$[36/-36/-36/-36]_s$	49.62	48.42
SCSF	$[90/70/-55/-55]_s$	61.94	61.53	$[-54/54/54/54]_s$	63.27	62.78
SSCF	$[-10/0/-5/25]_s$	64.84	64.50	$[-15/15/-15/15]_s$	64.12	63.87
SCCF	$[-10/65/-35/-35]_s$	69.88	69.34	$[-41/41/-41/41]_s$	70.84	69.37
CFCF	$[0/0/0/0]_s$	87.74	87.31	$[0/0/0/0]_s$	87.80	87.31
CSCF	$[0/0/0/0]_s$	90.28	89.80	$[0/0/0/0]_s$	90.41	89.80
CCCF	$[0/0/0/0]_s$	92.28	91.80	$[0/0/0/0]_s$	92.75	91.80
SSSS	$[90/90/90/90]_s$	159.9	159.09	$[90/90/90/90]_s$	159.80	159.09
SSSC	$[90/90/90/90]_s$	245.7	243.00	$[90/90/90/90]_s$	245.64	243.00
SSCC	$[90/90/90/90]_s$	246.4	243.64	$[90/90/90/90]_s$	246.50	243.64
SCSC	$[90/90/90/90]_s$	353.9	351.26	$[90/90/90/90]_s$	353.93	351.24
CCCS	$[90/90/90/90]_s$	247.1	244.45	$[90/90/90/90]_s$	247.32	244.45
CCCC	$[90/90/90/90]_s$	354.9	353.48	$[90/90/90/90]_s$	355.14	353.47

Similarly, frequency values of symmetric 8-layered composite plate are obtained for a/b=2 in Table 6.3. Although there is not much difference between present results and the results given by Narita (2003), the hybrid algorithm gives slightly better results than the other in some boundary conditions such as SSSF and SCSF. Additionally, these values have been compared with the results obtained by using the finite element method and similar results have achieved. It is understood from Tables 6.2 and 6.3 that algorithm and finite element code could yield reliable results. Both have a good agreement with previous study.

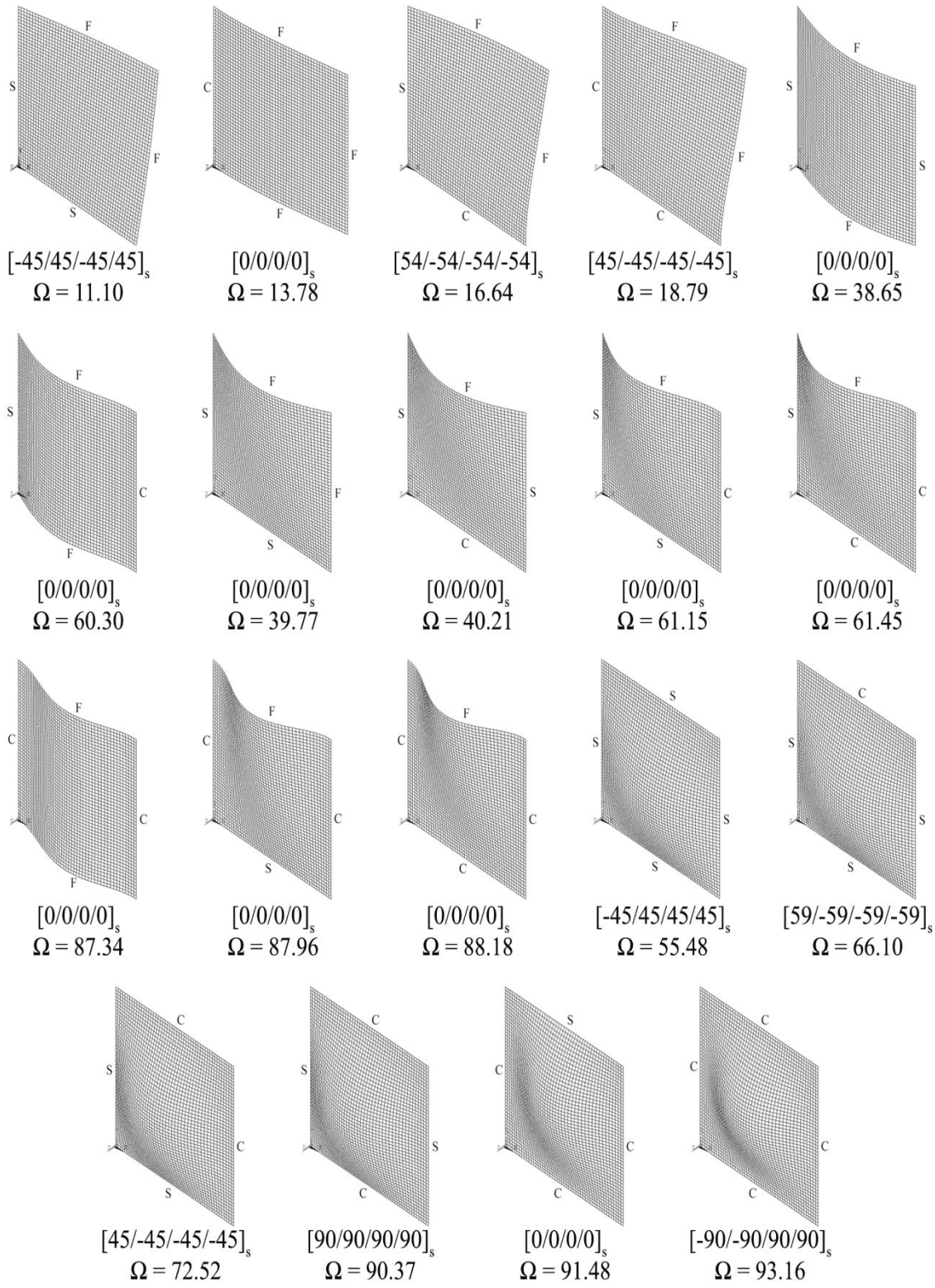

Figure 6.4. The mode shapes and fundamental frequencies Ω_{opt} for *a/b*=1

The vibration mode shapes corresponding to first natural frequency of laminated composite plate for various egde conditions are presented in Figures 6.4 and 6.5. Although the natural frequency parameters of composite plates increase in increasing aspect ratio, the corresponding mode shapes are similar to each other. It can be said that boundary conditions play a significiant role on mode shapes of laminated composite plates.

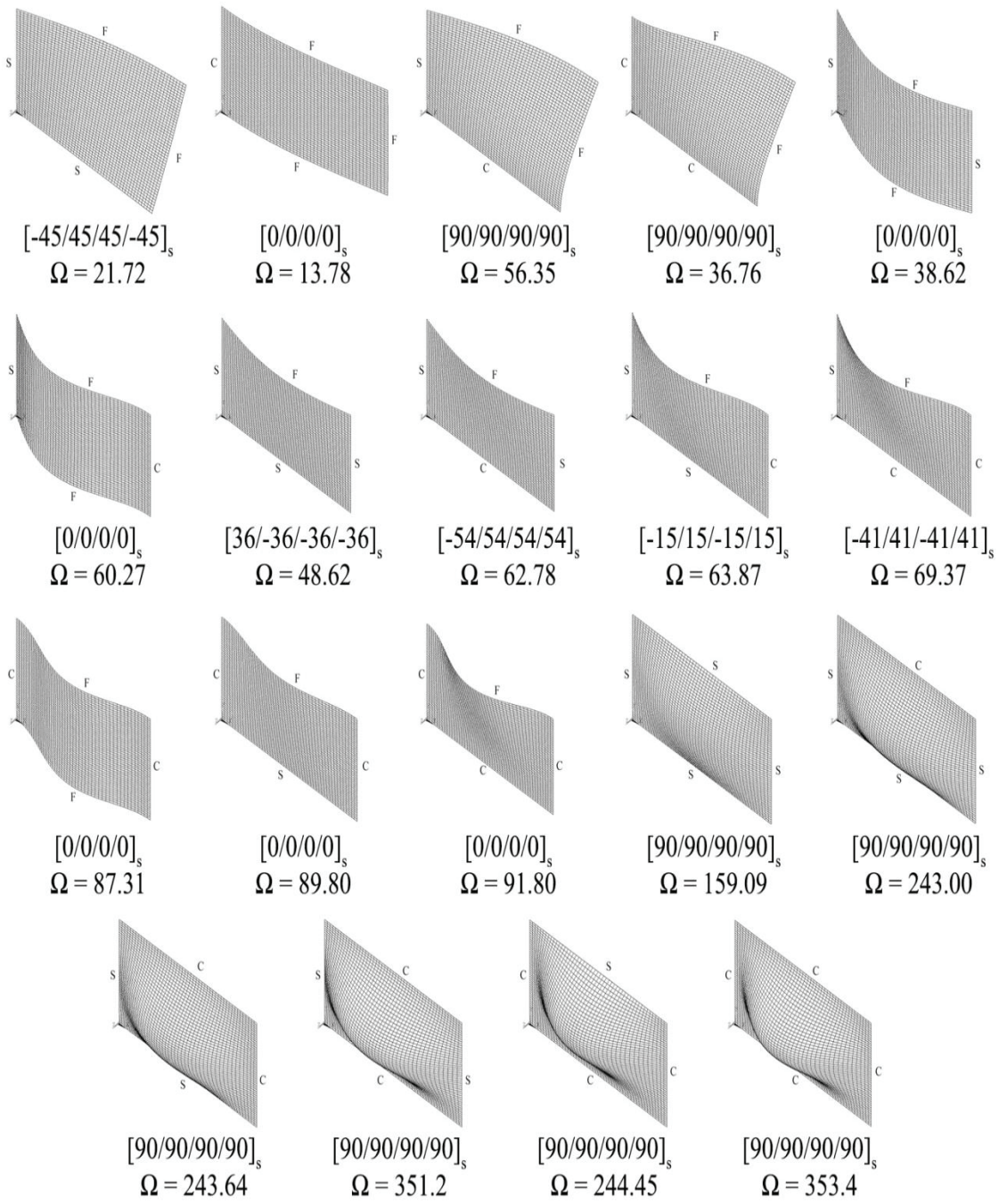

Figure 6.5. The mode shapes and fundamental frequencies Ω_{opt} for a/b=2

6.3. Optimization Results and Discussion

The optimum stacking sequences of composite plates which resist to vibration have been determined by using hybrid optimization algorithm (GA/GPSA). Then, the designs obtained from optimization results are compared with those of the finite element method. Non-dimensionalized frequency values of the plates have been presented in Tables 6.4-6.8.

As a first design problem, optimum designs have been investigated depending on various ply numbers *n = 4, 8, 16* in Tables 6.4-6.6, respectively. Table 6.4 shows the optimum designs for 4-layered composite plates. The results have been given in increasing aspect ratio *a/b = 1,2,3,4,5* and for different boundary conditions. The all fiber orientations have been taken as continous. As it can be understood from Table 6.4, the first natural frequency values increase with increasing aspect ratio. This fact not only accounts for the values in Table 6.4 but also in Table 6.5 and Table 6.6.

Table 6.4. Optimum stacking sequence for symmetric 4-layered composite plate

Boundary Conditions	a/b	Stacking Sequence	Ω_{opt} (GA/GPSA)	Ω_{opt} (FEM)
SSFF 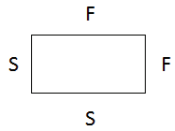	1	$[-45/45]_s$	11.920	10.823
	2	$[-45/45]_s$	22.558	20.456
	3	$[-45/45]_s$	35.762	32.203
	4	$[-45/45]_s$	47.683	45.899
	5	$[-45/45]_s$	59.604	56.726
CFFF 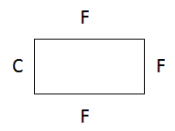	1	$[0/0]_s$	13.797	13.778
	2	$[0/0]_s$	13.797	13.772
	3	$[0/0]_s$	13.797	13.767
	4	$[0/0]_s$	13.797	13.763
	5	$[0/0]_s$	13.797	13.760
SCFF 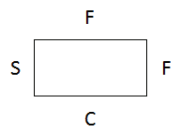	1	$[-54/54]_s$	17.229	16.912
	2	$[90/90]_s$	57.720	56.305
	3	$[90/90]_s$	125.762	124.746
	4	$[90/90]_s$	222.352	220.967
	5	$[90/90]_s$	346.535	342.381

(cont. on next page)

Table 6.4. (Cont.)

CCFF 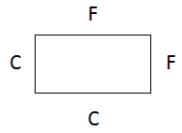	1	$[45/-45]_s$	19.167	18.368
	2	$[90/90]_s$	57.726	56.736
	3	$[90/90]_s$	126.686	125.084
	4	$[90/90_s$	223.261	220.389
	5	$[90/90]_s$	347.438	343.078
SFSF 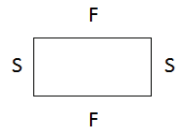	1	$[0/0]_s$	38.713	38.633
	2	$[0/0]_s$	38.713	38.602
	3	$[0/0]_s$	38.713	38.583
	4	$[0/0]_s$	38.713	38.576
	5	$[0/0]_s$	38.713	38.570
SFCF 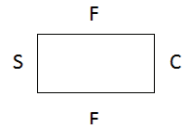	1	$[0/0]_s$	60.490	60.276
	2	$[0/0]_s$	60.490	60.245
	3	$[0/0]_s$	60.490	60.224
	4	$[0/0]_s$	60.490	60.210
	5	$[0/0]_s$	60.490	60.199
SSSF 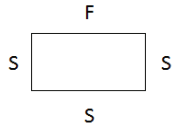	1	$[0/0]_s$	39.899	39.753
	2	$[36/-36]_s$	49.629	45.375
	3	$[-42/42]_s$	68.827	62.499
	4	$[-43/43]_s$	89.391	84.917
	5	$[44/-44]_s$	110.408	103.322
SCSF 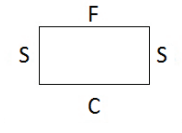	1	$[0/0]_s$	40.625	40.198
	2	$[-54/54]_s$	63.275	60.479
	3	$[-90/90]_s$	129.508	128.719
	4	$[-90/90]_s$	225.975	223.964
	5	$[-90/90]_s$	350.100	345.597
SSCF 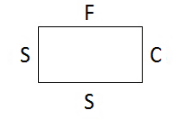	1	$[0/0]_s$	61.381	61.150
	2	$[15/-15]_s$	64.128	63.926
	3	$[-37/37]_s$	79.553	72.820
	4	$[41/-41]_s$	100.139	96.749
	5	$[-43/43]_s$	121.989	117.904
SCCF 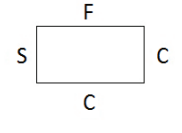	1	$[0/0]_s$	61.917	61.427
	2	$[-41/41]_s$	70.848	69.279
	3	$[90/90]_s$	130.842	129.782
	4	$[90/90]_s$	227.096	224.715
	5	$[90/90]_s$	351.119	346.202
CFCF 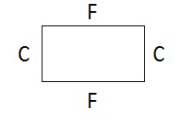	1	$[0/0]_s$	87.804	87.297
	2	$[0/0]_s$	87.804	87.268
	3	$[0/0]_s$	87.804	87.248
	4	$[0/0]_s$	87.804	87.231
	5	$[0/0]_s$	87.804	87.217

(cont. on next page)

Table 6.4. (Cont.)

CSCF 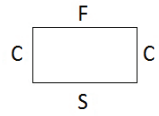	1	$[0/0]_s$	88.464	87.922
	2	$[0/0]_s$	90.415	89.756
	3	$[23/-23]_s$	94.930	91.596
	4	$[-36/36]_s$	111.389	107.059
	5	$[40/-40]_s$	132.015	127.533
CCCF 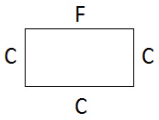	1	$[0/0]_s$	88.858	88.144
	2	$[0/0]_s$	92.752	91.756
	3	$[90/90]_s$	132.237	131.173
	4	$[90/90]_s$	228.081	225.668
	5	$[90/90]_s$	351.905	347.917
SSSS 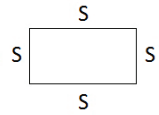	1	$[-45/45]_s$	56.498	54.618
	2	$[90/90]_s$	159.804	159.015
	3	$[90/90]_s$	353.244	350.887
	4	$[90/90]_s$	624.194	620.127
	5	$[90/90]_s$	972.596	969.591
SSSC 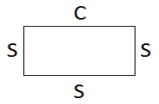	1	$[-59/59]_s$	67.061	64.742
	2	$[90/90]_s$	245.648	243.006
	3	$[90/90]_s$	548.004	545.895
	4	$[90/90]_s$	971.402	968.458
	5	$[90/90]_s$	1515.848	1512.985
SSCC 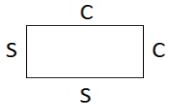	1	$[-45/45]_s$	73.454	70.743
	2	$[90/90]_s$	246.504	243.524
	3	$[90/90]_s$	548.708	547.581
	4	$[90/90]_s$	972.052	967.318
	5	$[90/90]_s$	1516.425	1489.325
SCSC 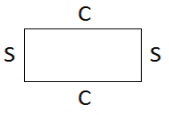	1	$[90/90]_s$	90.897	90.375
	2	$[90/90]_s$	353.938	351.480
	3	$[90/90]_s$	792.888	783.296
	4	$[90/90]_s$	1407.523	1982.761
	5	$[90/90]_s$	2197.725	2133.252
CCCS 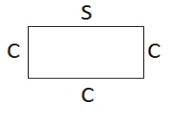	1	$[0/0]_s$	92.075	91.483
	2	$[90/90]_s$	247.322	244.331
	3	$[90/90]_s$	549.237	546.084
	4	$[90/90]_s$	972.477	966.553
	5	$[90/90]_s$	1516.830	1483.813
CCCC 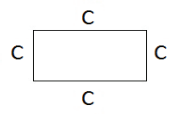	1	$[90/90]_s$	93.694	93.120
	2	$[90/90]_s$	355.144	353.475
	3	$[90/90]_s$	793.783	789.657
	4	$[90/90]_s$	1408.325	1396.968
	5	$[90/90]_s$	2198.540	2123.589

The optimum designs of laminated composite plates for the number of ply *n=8* are shown in Table 6.5. It is seen that all fiber oriantation and the natural frequency values are the same with the results of ply, *n=4*.

Table 6.5. Optimum stacking sequence for symmetric 8-layered composite plate

Boundary Conditions	a/b	Stacking Sequence	Ω_{opt} (GA/GPSA)	Ω_{opt} (FEM)
SSFF 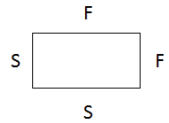	1	$[-45/45/-45/45]_s$	11.920	11.104
	2	$[-45/45/45/-45]_s$	22.558	21.728
	3	$[-45/45/45/-45]_s$	35.762	32.762
	4	$[-45/45/45/-45]_s$	47.683	44.961
	5	$[-45/45/45/-45]_s$	59.604	55.837
CFFF 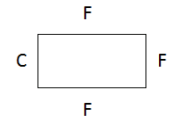	1	$[0/0/0/0]_s$	13.797	13.785
	2	$[0/0/0/0]_s$	13.797	13.781
	3	$[0/0/0/0]_s$	13.797	13.774
	4	$[0/0/0/0]_s$	13.797	13.770
	5	$[0/0/0/0]_s$	13.797	13.767
SCFF 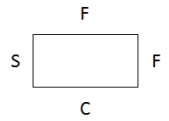	1	$[54/-54/-54/-54]_s$	17.229	16.645
	2	$[90/90/90/90]_s$	57.720	56.760
	3	$[90/90/90/90]_s$	125.762	124.885
	4	$[90/90/90/90]_s$	222.352	220.317
	5	$[90/90/90/90]_s$	346.535	342.104
CCFF 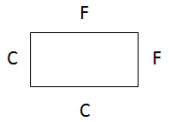	1	$[45/-45/-45/-45]_s$	19.167	18.790
	2	$[90/90/90/90]_s$	57.726	56.765
	3	$[90/90/90/90]_s$	126.686	125.147
	4	$[90/90/90/90]_s$	223.261	220.501
	5	$[90/90/90/90]_s$	347.438	343.251
SFSF 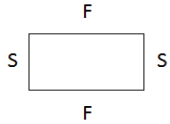	1	$[0/0/0/0]_s$	38.713	38.652
	2	$[0/0/0/0]_s$	38.713	38.621
	3	$[0/0/0/0]_s$	38.713	38.603
	4	$[0/0/0/0]_s$	38.713	38.595
	5	$[0/0/0/0]_s$	38.713	38.590

(cont. on next page)

Table 6.5. (Cont.)

SFCF 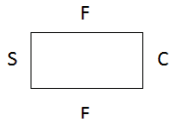	1	$[0/0/0/0]_s$	60.490	60.306
	2	$[0/0/0/0]_s$	60.490	60.275
	3	$[0/0/0/0]_s$	60.490	60.255
	4	$[0/0/0/0]_s$	60.490	60.240
	5	$[0/0/0/0]_s$	60.490	60.229
SSSF 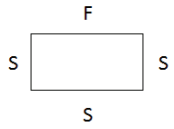	1	$[0/0/0/0]_s$	39.899	39.773
	2	$[36/-36/-36/-36]_s$	49.629	47.429
	3	$[-42/42/42/42]_s$	68.827	65.113
	4	$[-43/43/43/43]_s$	89.391	84.605
	5	$[44/-44/-44/-44]_s$	110.408	104.776
SCSF 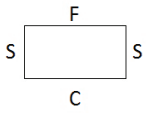	1	$[0/0/0/0]_s$	40.625	40.219
	2	$[-54/54/54/54]_s$	63.275	62.781
	3	$[-90/90/90/-90]_s$	129.508	128.784
	4	$[-90/90/90/-90]_s$	225.975	224.077
	5	$[-90/90/90/-90]_s$	350.100	345.773
SSCF 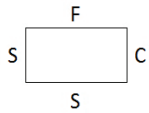	1	$[0/0/0/0]_s$	61.381	61.150
	2	$[-15/15/-15/15]_s$	64.128	63.870
	3	$[-37/37/37/37]_s$	79.553	77.234
	4	$[41/-41/41/-41]_s$	100.139	95.187
	5	$[-43/43/43/43]_s$	121.989	117.866
SCCF 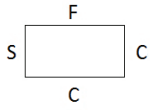	1	$[0/0/0/0]_s$	61.917	61.458
	2	$[-41/41/-41/41]_s$	72.898	70.376
	3	$[-90/-90/-90/-90]_s$	130.842	129.848
	4	$[-90/90/90/90]_s$	227.096	224.829
	5	$[-90/90/90/90]_s$	351.119	347.378
CFCF 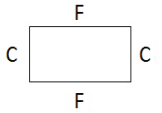	1	$[0/0/0/0]_s$	87.804	87.342
	2	$[0/0/0/0]_s$	87.804	87.312
	3	$[0/0/0/0]_s$	87.804	87.292
	4	$[0/0/0/0]_s$	87.804	87.276
	5	$[0/0/0/0]_s$	87.804	87.261
CSCF 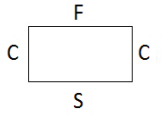	1	$[0/0/0/0]_s$	88.464	87.967
	2	$[0/0/0/0]_s$	90.415	89.801
	3	$[23/-23/-23/-23]_s$	94.930	92.176
	4	$[-36/36/36/36]_s$	111.389	107.063
	5	$[40/-40/-40/-40]_s$	132.015	125.300

(cont. on next page)

Table 6.5. (Cont.)

CCCF 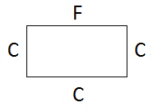	1	$[0/0/0/0]_s$	88.858	88.189
	2	$[0/0/0/0]_s$	92.752	91.800
	3	$[90/90/90/90]_s$	132.237	131.240
	4	$[90/90/90/90]_s$	228.081	226.783
	5	$[90/90/90/90]_s$	351.905	348.093
SSSS 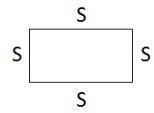	1	$[-45/45/45/45]_s$	56.498	55.486
	2	$[90/90/90/90]_s$	159.804	159.095
	3	$[90/90/90/90]_s$	353.244	350.065
	4	$[90/90/90/90]_s$	624.194	617.438
	5	$[90/90/90/90]_s$	972.596	960.207
SSSC 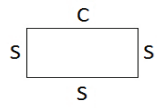	1	$[59/-59/-59/-59]_s$	67.061	66.100
	2	$[90/90/90/90]_s$	245.648	243.006
	3	$[90/90/90/90]_s$	548.004	541.130
	4	$[90/90/90/90]_s$	971.402	962.164
	5	$[90/90/90/90]_s$	1515.848	1492.233
SSCC 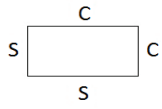	1	$[45/-45/-45/-45]_s$	73.454	72.528
	2	$[90/90/90/90]_s$	246.504	243.647
	3	$[90/90/90/90]_s$	548.708	542.533
	4	$[90/90/90/90]_s$	972.052	967.234
	5	$[90/90/90/90]_s$	1516.425	1493.825
SCSC 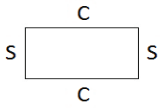	1	$[90/90/90/90]_s$	90.897	90.371
	2	$[90/90/90/90]_s$	353.938	351.248
	3	$[90/90/90/90]_s$	792.888	788.048
	4	$[90/90/90/90]_s$	1407.523	1385.961
	5	$[90/90/90/90]_s$	2197.725	2056.152
CCCS 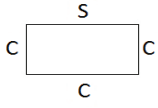	1	$[0/0/0/0]_s$	92.075	91.489
	2	$[90/90/90/90]_s$	247.322	244.455
	3	$[90/90/90/90]_s$	549.237	546.084
	4	$[90/90/90/90]_s$	972.477	962.553
	5	$[90/90/90/90]_s$	1516.830	1493.113
CCCC 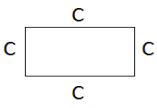	1	$[90/90/90/90]_s$	93.694	93.167
	2	$[90/90/90/90]_s$	355.144	353.475
	3	$[90/90/90/90]_s$	793.783	785.656
	4	$[90/90/90/90]_s$	1408.325	1389.968
	5	$[90/90/90/90]_s$	2198.540	2045.936

Optimum fiber orientations for symmetric 16-layered composite plate in the increasing aspect ratio and subjected to different boundary conditions have been presented in Table 6.6.

Table 6.6. Optimum stacking sequence for symmetric 16-layered composite plate

Boundary Conditions	a/b	Stacking Sequence	Ω_{opt} (GA/GPSA)	Ω_{opt} (FEM)
SSFF 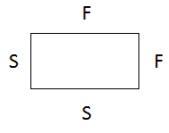	1	$[-45/45/-45/45/-45/45/-45/45]_s$	11.920	11.125
	2	$[-45/45/-45/45/-45/45/-45/45]_s$	22.558	21.983
	3	$[-45/45/45/45/45/45/45/-45]_s$	35.762	32.936
	4	$[-45/45/45/45/45/45/45/-45]_s$	47.683	43.968
	5	$[-45/45/45/45/45/45/45/-45]_s$	59.604	54.840
CFFF 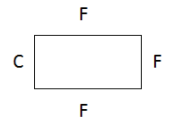	1	$[0/0/0/0/0/0/0/0]_s$	13.797	13.785
	2	$[0/0/0/0/0/0/0/0]_s$	13.797	13.779
	3	$[0/0/0/0/0/0/0/0]_s$	13.797	13.774
	4	$[0/0/0/0/0/0/0/0]_s$	13.797	13.770
	5	$[0/0/0/0/0/0/0/0]_s$	13.797	13.767
SCFF 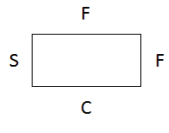	1	$[54/-54/-54/-54/-54/-54/-54/-54]_s$	17.229	16.736
	2	$[90/90/90/90/90/90/90/90]_s$	57.720	56.950
	3	$[90/90/90/90/90/90/90/90]_s$	125.762	124.885
	4	$[90/90/90/90/90/90/90/90]_s$	222.352	220.317
	5	$[90/90/90/90/90/90/90/90]_s$	346.535	342.104
CCFF 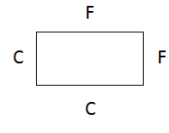	1	$[45/-45/-45/-45/-45/-45/-45/-45]_s$	19.167	18.850
	2	$[90/90/90/90/90/90/90/90]_s$	57.726	56.765
	3	$[90/90/90/90/90/90/90/90]_s$	126.686	125.147
	4	$[90/90/90/90/90/90/90/90]_s$	221.835	220.501
	5	$[90/90/90/90/90/90/90/90]_s$	347.438	342.251
SFSF 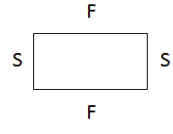	1	$[0/0/0/0/0/0/0/0]_s$	38.713	38.652
	2	$[0/0/0/0/0/0/0/0]_s$	38.713	38.621
	3	$[0/0/0/0/0/0/0/0]_s$	38.713	38.603
	4	$[0/0/0/0/0/0/0/0]_s$	38.713	38.595
	5	$[0/0/0/0/0/0/0/0]_s$	38.713	38.590

(cont. on next page)

Table 6.6. (Cont.)

SFCF 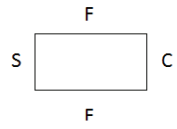	1	$[0/0/0/0/0/0/0/0]_s$	60.490	60.306
	2	$[0/0/0/0/0/0/0/0]_s$	60.490	60.275
	3	$[0/0/0/0/0/0/0/0]_s$	60.490	60.255
	4	$[0/0/0/0/0/0/0/0]_s$	60.490	60.240
	5	$[0/0/0/0/0/0/0/0]_s$	60.490	60.229
SSSF 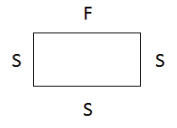	1	$[0/0/0/0/0/0/0/0]_s$	39.899	39.773
	2	$[36/-36/-36/-36/-36/-36/-36/-36]_s$	49.629	48.563
	3	$[-42/42/42/42/42/42/42/42]_s$	68.827	65.512
	4	$[-43/43/43/43/43/43/43/43]_s$	89.391	85.692
	5	$[44/-44/-44/-44/-44/-44/-44/-44]_s$	110.408	107.332
SCSF 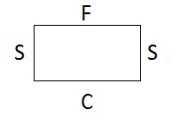	1	$[0/0/0/0/0/0/0/0]_s$	40.625	40.219
	2	$[-54/54/54/54/54/54/54/54]_s$	63.275	62.885
	3	$[-90/90/90/90/90/90/90/-90]_s$	129.508	128.784
	4	$[90/90/90/90/90/90/90/90]_s$	225.975	224.077
	5	$[90/90/90/90/90/90/90/90]_s$	350.100	348.773
SSCF 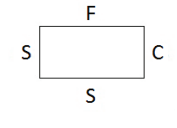	1	$[0/0/0/0/0/0/0/0]_s$	61.381	61.150
	2	$[15/-15/-15/-15/-15/-15/-15/-15]_s$	64.128	64.264
	3	$[-37/37/37/37/37/37/37/37]_s$	79.553	78.700
	4	$[41/-41/41/-41/-41/-41/-41/-41]_s$	100.139	96.429
	5	$[-43/43/43/43/43/43/43/43]_s$	121.989	119.541
SCCF 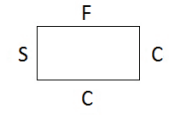	1	$[0/0/0/0/0/0/0/0]_s$	61.917	61.458
	2	$[-41/41/41/41/41/41/41/41]_s$	70.848	69.710
	3	$[90/90/90/90/90/90/90/90]_s$	130.842	129.884
	4	$[-90/90/90/90/90/90/90/90]_s$	227.096	224.836
	5	$[-90/90/90/90/90/90/90/90]_s$	351.119	346.378
CFCF 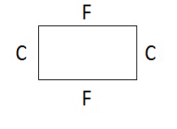	1	$[0/0/0/0/0/0/0/0]_s$	87.804	87.342
	2	$[0/0/0/0/0/0/0/0]_s$	87.804	87.312
	3	$[0/0/0/0/0/0/0/0]_s$	87.804	87.292
	4	$[0/0/0/0/0/0/0/0]_s$	87.804	87.276
	5	$[0/0/0/0/0/0/0/0]_s$	87.804	87.261
CSCF 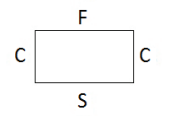	1	$[0/0/0/0/0/0/0/0]_s$	88.464	87.967
	2	$[0/0/0/0/0/0/0/0]_s$	90.415	89.801
	3	$[23/-23/-23/-23/-23/-23/-23/-23]_s$	94.930	92.892
	4	$[-36/36/36/36/36/36/36/36]_s$	111.389	108.300
	5	$[40/-40/-40/-40/-40/-40/-40/-40]_s$	132.015	128.918

(cont. on next page)

Table 6.6. (Cont.)

CCCF 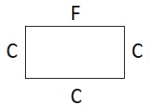	1	$[0/0/0/0/0/0/0/0]_s$	88.858	88.189
	2	$[0/0/0/0/0/0/0/0]_s$	92.752	91.800
	3	$[90/90/90/90/90/90/90/90]_s$	132.237	131.240
	4	$[90/90/90/90/90/90/90/90]_s$	228.081	226.783
	5	$[90/90/90/90/90/90/90/90]_s$	351.905	348.093
SSSS 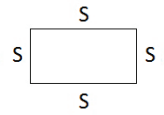	1	$[-45/45/45/45/45/45/45/45]_s$	56.498	55.714
	2	$[90/90/90/90/90/90/90/90]_s$	159.804	159.095
	3	$[90/90/90/90/90/90/90/90]_s$	353.244	350.065
	4	$[90/90/90/90/90/90/90/90]_s$	624.194	618.438
	5	$[90/90/90/90/90/90/90/90]_s$	972.596	965.207
SSSC 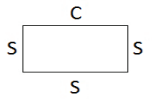	1	$[-59/59/59/59/59/59/59/59]_s$	67.061	66.460
	2	$[90/90/90/90/90/90/90/90]_s$	245.648	243.006
	3	$[90/90/90/90/90/90/90/90]_s$	548.004	541.130
	4	$[90/90/90/90/90/90/90/90]_s$	971.402	942.164
	5	$[90/90/90/90/90/90/90/90]_s$	1515.848	1452.233
SSCC 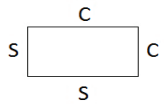	1	$[-45/45/45/45/45/45/45/45]_s$	73.454	72.784
	2	$[90/90/90/90/90/90/90/90]_s$	246.504	243.647
	3	$[90/90/90/90/90/90/90/90]_s$	548.708	538.533
	4	$[90/90/90/90/90/90/90/90]_s$	972.052	937.234
	5	$[90/90/90/90/90/90/90/90]_s$	1516.425	1453.825
SCSC 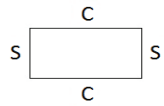	1	$[90/90/90/90/90/90/90/90]_s$	90.897	90.371
	2	$[90/90/90/90/90/90/90/90]_s$	353.938	351.148
	3	$[90/90/90/90/90/90/90/90]_s$	792.888	768.048
	4	$[90/90/90/90/90/90/90/90]_s$	1407.523	1315.961
	5	$[90/90/90/90/90/90/90/90]_s$	2197.725	2076.152
CCCS 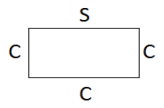	1	$[0/0/0/0/0/0/0/0]_s$	92.075	91.489
	2	$[90/90/90/90/90/90/90/90]_s$	247.322	244.455
	3	$[90/90/90/90/90/90/90/90]_s$	549.237	536.084
	4	$[90/90/90/90/90/90/90/90]_s$	972.477	952.553
	5	$[90/90/90/90/90/90/90/90]_s$	1516.830	1453.113
CCCC 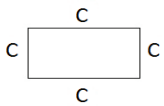	1	$[90/90/90/90/90/90/90/90]_s$	93.694	93.167
	2	$[90/90/90/90/90/90/90/90]_s$	355.144	353.475
	3	$[90/90/90/90/90/90/90/90]_s$	793.783	775.656
	4	$[90/90/90/90/90/90/90/90]_s$	1408.325	1369.968
	5	$[90/90/90/90/90/90/90/90]_s$	2198.540	2077.623

It can be understood from Tables 6.4-6.6 that, as the plate aspect ratio increases, the first natural frequency values of composite plates increase. It can also be seen from Table 6.4-6.6 how the boundary conditions affect the natural frequency of composite plate in detail. Similarly, when the number of clamped in boundary condition of plate increases, first natural frequency values of composite plate increase considerably. Such as Ω = 11.920 for boundary condition SSFF whereas Ω = 93.694 for boundary condition CCCC. The plate have capability of more free transverse vibration in simply supported (S) and free (F) boundary conditions, and the bending effect becomes the most important factor. Therefore, lower frequency values are obtained in these boundary conditions. The optimal fiber oriantations change between 0 and 90 or 0 and -90 with the increase in a/b ratios depending on the boundary conditions, which have smooth transional region for the simply supported case, such as SSSF. If it is for the case of clamped boundary condition, the optimal fiber oriantations have a sudden manner, such as CCCS and CCCC. Tables 6.4-6.6 also shows effect of number of layers on the optimum designs. As mentioned briefly in the previous comments, the maximum natural frequency and the optimum fiber oriantations are not influenced from increasing number of layers at constant thickness.

As additional study, the effect of different material on the vibration behavior of the laminated composite structure is investigated. The degree of orthotropy (E_1/E_2) has been taken as a parameter. The longitudinal young's modulus E_1 is property of elaticity which is parallel to the fibers, the transverse young's modulus E_2 is perpendicular direction to the fiber. Some boundary conditions, SSSF, SSCF, CSCF, SCSF, SCCF, having different fiber orientation angles in increasing aspect ratio have been chosen. The results for symmetric 8-layered composite plate with selected boundary conditions and aspect ratios a/b = *1, 2* are given in Table 6.7. Both longitudinal and transverse young's modulus affects the total stiffness of composite structure. However, longitudinal young's modulus greatly contribute to the stiffness because it is in the direction of fiber. It is seen that, when rate in orthotropy degree of material is increased, maximum natural frequency values increase. It is clear from the results that the rate of E_1/E_2 is one of the primary properties considered when selecting a material to stiffen the structure.

Table 6.7. Effect of degree of orthotropy for symmetric 8-layered composite plate

BC's	a/b	E_1/E_2	Stacking Sequence	Ω_{opt} (GA/GPSA)	Ω_{opt} (FEM)
SSSF	1	5	$[0/0/0/0]_s$	22.725	22.647
		10	$[0/0/0/0]_s$	32.147	32.061
		15	$[0/0/0/0]_s$	39.375	39.253
		20	$[0/0/0/0]_s$	45.468	45.308
	2	5	$[38/-38/-38/-38]_s$	29.104	27.762
		10	$[37/-37/-37/-37]_s$	40.291	38.491
		15	$[36/-36/-36/-36]_s$	48.998	46.824
		20	$[36/-36/-36/-36]_s$	56.378	53.874
SSCF	1	5	$[0/0/0/0]_s$	34.967	34.812
		10	$[0/0/0/0]_s$	49.457	49.276
		15	$[0/0/0/0]_s$	60.575	60.348
		20	$[0/0/0/0]_s$	69.947	69.673
	2	5	$[37/-37/-37/-37]_s$	36.882	33.922
		10	$[17/-17/-17/-17]_s$	51.762	50.310
		15	$[-15/15/15/15]_s$	63.290	61.716
		20	$[14/-14/-14/-14]_s$	73.034	71.313
CSCF	1	5	$[0/0/0/0]_s$	50.399	50.081
		10	$[0/0/0/0]_s$	71.280	70.880
		15	$[0/0/0/0]_s$	87.302	86.612
		20	$[0/0/0/0]_s$	100.809	100.239
	2	5	$[0/0/0/0]_s$	51.497	51.129
		10	$[0/0/0/0]_s$	72.847	72.374
		15	$[0/0/0/0]_s$	89.227	88.624
		20	$[0/0/0/0]_s$	103.035	102.303
SCSF	1	5	$[0/0/0/0]_s$	23.241	23.100
		10	$[0/0/0/0]_s$	32.769	32.511
		15	$[0/0/0/0]_s$	40.094	39.698
		20	$[0/0/0/0]_s$	46.274	45.794
	2	5	$[52/-52/-52/-52]_s$	38.491	37.943
		10	$[53/-53/-53/-53]_s$	53.075	51.985
		15	$[-54/54/54/54]_s$	64.447	62.986
		20	$[-54/54/54/54]_s$	74.095	72.246

(cont. on next page)

Table 6.7. (Cont.)

SCCF	1	5	$[0/0/0/0]_s$	35.330	35.121
		10	$[0/0/0/0]_s$	49.910	49.589
		15	$[0/0/0/0]_s$	61.105	60.657
		20	$[0/0/0/0]_s$	70.545	69.979
	2	5	$[42/-42/-42/-42]_s$	43.308	42.188
		10	$[-41/41/41/41]_s$	59.400	56.494
		15	$[41/-41/-41/-41]_s$	71.982	69.438
		20	$[41/-41/-41/-41]_s$	82.670	79.581

Fiber angles in the stacking sequences of the laminated composites have been taken as continuous in this study and the optimization has been done by considering this assumption. However, conventional designs are mainly used in the industry due to their economic production methods. In order to show the advantage of studying with continuous design variables, the typical stacking sequences are chosen to investigate the effect of conventional and continuous designs on natural frequency of composite plate. These are specially orthotropic $[0/0/0/0]_s$, $[0/90/0/90]_s$ and the alternating angle-ply sequence $[30/-30/30/-30]_s$, $[45/-45/45/-45]_s$ and the quasi – isotropic $[0/-45/45/90]_s$. They have been presented together in Table 6.8. The optimum composite plate orientations for continuous designs are shown in grey color. Number of layer and a/b are taken 8 and 2, respectively.

Table 6.8. The comparison between conventional and continuous designs for symmetrical 8-layered composite plate

Boundary Conditions	Stacking Sequence	Ω_{opt}	Ω_{opt} (FEM)
SSSF 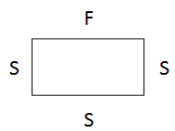	$[0/0/0/0]_s$	43.262	43.027
	$[0/90/0/90]_s$	37.863	37.737
	$[30/-30/30/-30]_s$	49.123	47.582
	$[45/-45/45/-45]_s$	48.580	46.784
	$[0/-45/45/90]_s$	45.256	44.220
	$[36/-36/-36/-36]_s$	49.629	47.429

(cont. on next page)

Table 6.8. (Cont.)

SCSF 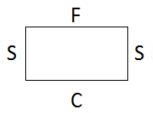	$[0/0/0/0]_s$	47.475	46.798
	$[0/90/0/90]_s$	52.019	51.795
	$[30/-30/30/-30]_s$	59.114	55.770
	$[45/-45/45/-45]_s$	62.414	61.306
	$[0/-45/45/90]_s$	55.194	53.307
	$[-54/54/54/54]_s$	63.275	62.781
SSCF 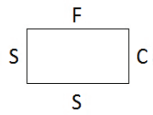	$[0/0/0/0]_s$	63.980	63.732
	$[0/90/0/90]_s$	54.993	54.852
	$[30/-30/30/-30]_s$	63.107	58.785
	$[45/-45/45/-45]_s$	58.097	53.723
	$[0/-45/45/90]_s$	61.222	61.009
	$[-15/15/-15/-15]_s$	64.128	63.870
SCCF 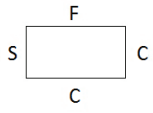	$[0/0/0/0]_s$	67.128	66.462
	$[0/90/0/90]_s$	65.780	65.614
	$[30/-30/30/-30]_s$	70.899	65.304
	$[45/-45/45/-45]_s$	71.767	67.600
	$[0/-45/45/90]_s$	69.410	68.439
	$[-41/41/-41/-41]_s$	72.898	70.376
CSCF 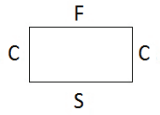	$[0/0/0/0]_s$	90.415	89.801
	$[0/90/0/90]_s$	76.955	76.775
	$[30/-30/30/-30]_s$	81.157	78.745
	$[45/-45/45/-45]_s$	69.681	66.954
	$[0/-45/45/90]_s$	81.973	80.742
	$[0/0/0/0]_s$	90.415	89.801

In Table 6.8, it is observed that it is possible to obtain more stiffened plate by using continuous designs. It is known that the conventional designs are mainly preferred due to the manufacturing ease but the results show that the continuous designs provide significant vibration resistant.

The effects of stacking sequences between conventional and continuous designs are also shown graphically for symmetric 8-layered composite plates with various aspect ratios in Figure 6.6. The results show that continuous designs of stacking sequences and dimensions of composite plates are significant parameter in design of laminated composite material in terms of maximum vibration behavior. Consequently, structural design engineer who does not realize the importance of continuous design variables on vibration behavior of structure may choose a stacking sequence which is far away from the optimum.

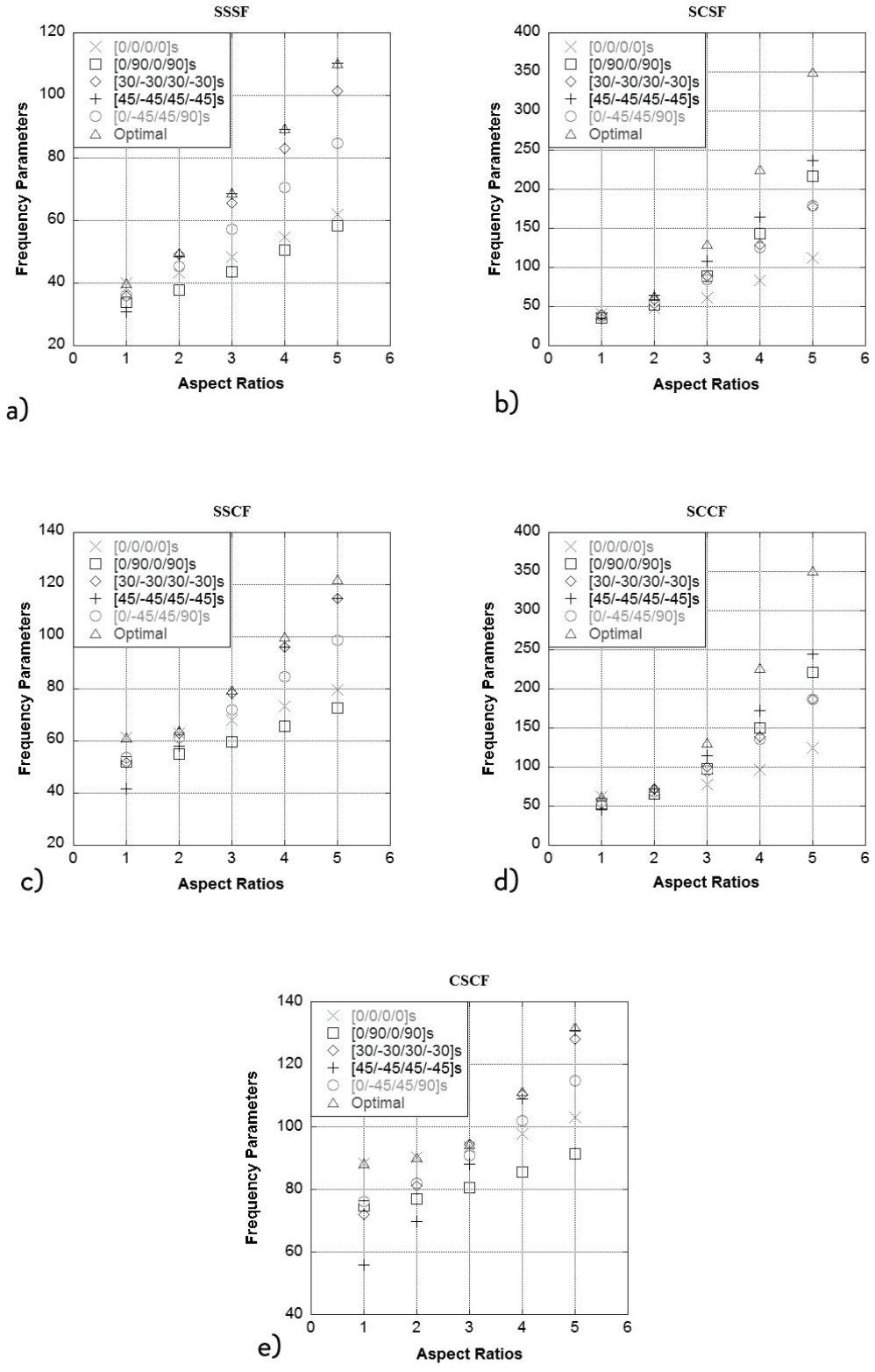

Figure 6.6. Comparison of the optimum frequency Ω_{opt} of symmetric 8-layered composite plate between conventional and continuous designs for different aspect ratios

The performmance of the hybrid algorithm is shown by comparing with the GA in Figure 6.7 and it shows the good efficiency of the hybrid algorithm. The optimal values for GA converge in the generation of 13 and 15 with around the initial population of 40 and 60, respectively. The GA parameters such as crossover rate and mutation rate also are selected to be 0.6 and 0.02, respectively. In addition, it is concluded that using of the hybrid algorithm provides a much higher convergence and reduced the CPU time in comparison with the GA.

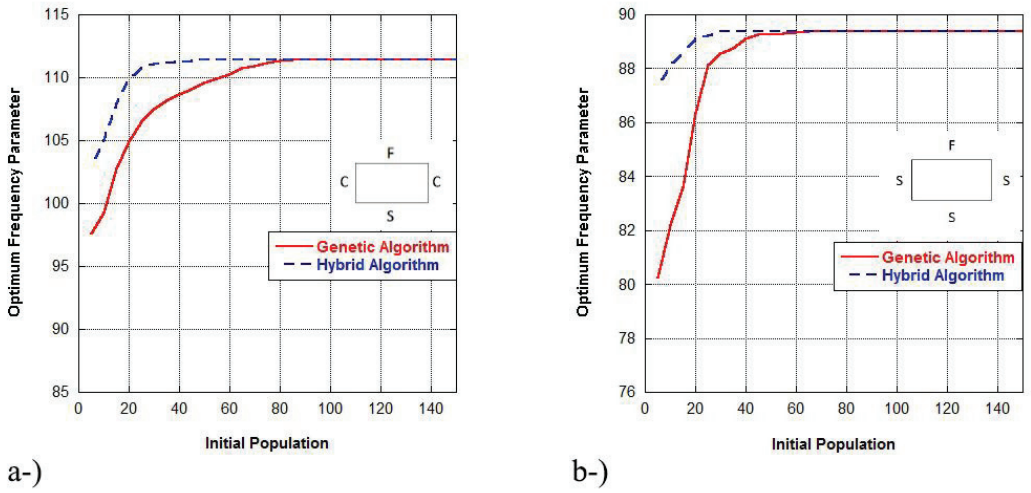

Figure 6.7. Comparison of the hybrid algorithm and GA results for symmetrical laminated rectangular plates having CSCF and SSSF edge conditions (a/b=4)

The best and mean fitness values of objective functions for SSCF boundary conditions and a/b = 1, 2, 3, 4, 5 design cases at each generation can be seen in Figure 6.8. The best fitness value corresponds to natural frequency (objective function) value and mean fitness value is the average of fitness values at each generation. The number of generations specifies the time when GA is to be stopped and is taken as 1000 for each design case. It is observed from the figures that the best fitness values improve more slowly in later generations and converge to the optimal point.

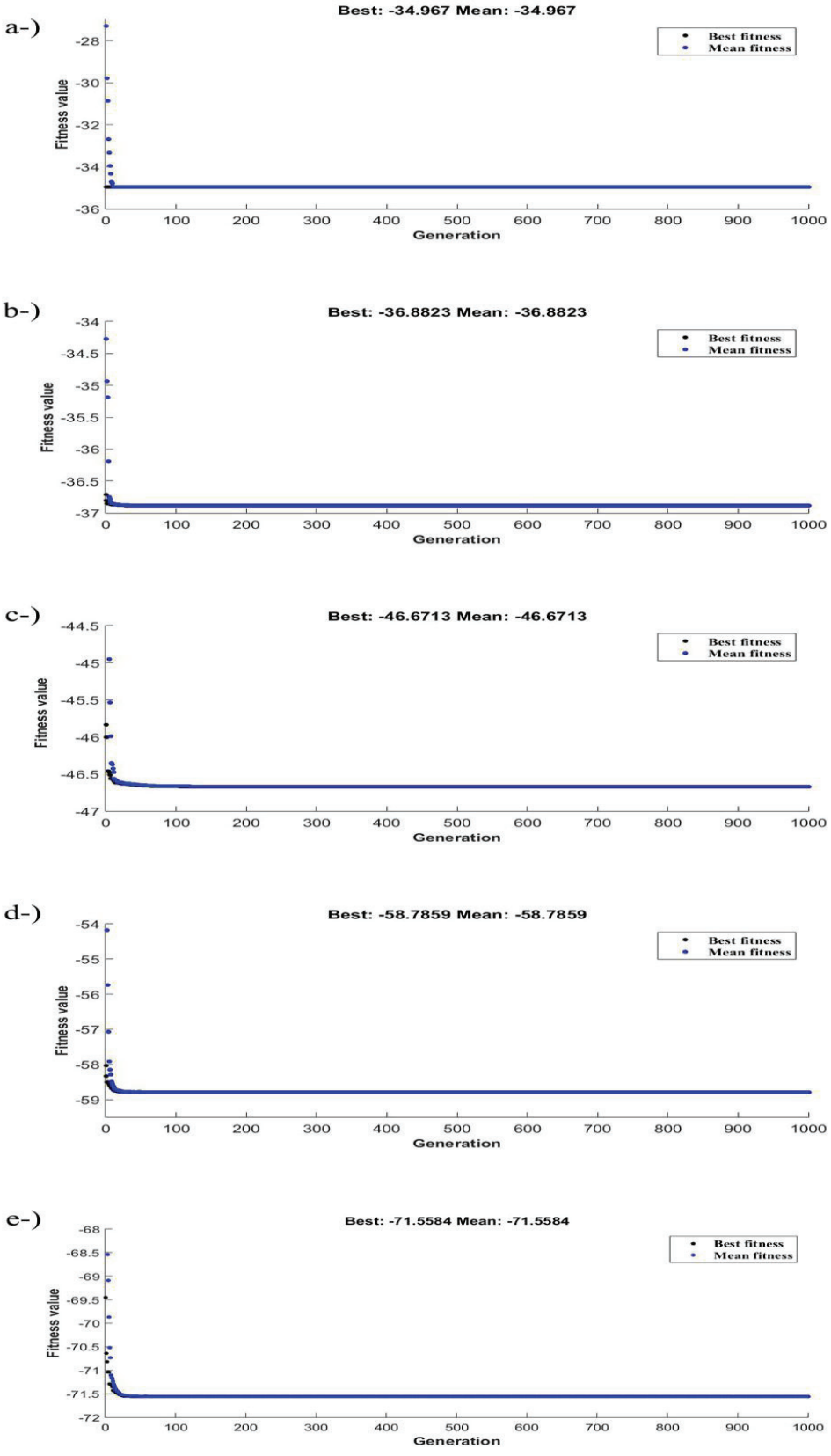

Figure 6.8. The best and mean values of the objective functions at each generation in GA for (a) a/b=1, (b) a/b=2, (c) a/b=3, (d) a/b=4, (e) a/b=5

CHAPTER 7

CONCLUSIONS

In this thesis, the optimum stacking sequence designs of laminated composite plates made of graphite/epoxy have been investigated in different fiber angle domains for maximum vibration resistance. A hybrid algorithm combining genetic algorithm and generalized pattern search algorihm is used in the optimization to obtain higher performance and improve the quality of solutions. MATLAB Global Optimization and Symbolic Math Toolboxes have been utilized in optimization process. The optimization has been performed in various combinations of boundary conditions, which are simply supported, free and clamped on different plate edges; aspect ratios ($a/b = 1, 2, 3, 4, 5$), the number of plies ($n = 4, 8, 16$), degree of material orthotropy ($E_1/E_2 = 5, 10, 15, 20$) by maximizing the first natural frequency of laminated composite plates for each case. In order to increase the reliability of optimization process, genetic algorithm is run 30 times and stopped after 1000 evaluations at every turn. Analytically, the Rayleigh-Ritz method has been employed to analyze the free vibration of a symmetrically laminated composite rectangular plate with various boundary conditions. Free vibration equation is taken as objective function and fiber angles of the laminated composite plates are considered as continuous design variables. The optimum designs obtained for maximized vibration behavior have also been verified by the finite element technique. Modal analysis of laminated composite structure have been carried out by using the software package ANSYS 14.0 and mode shapes of composite plates as well as the natural frequencies have been found out at the end of modal analysis. Mode shapes have been observed for careful examination of deformation.

Before optimization process, the verification of algorithms is very important to ensure that optimum results are safely achieved. Therefore, the accuracy of the natural frequency parameter and optimization algorithm are checked by using the study in the literature. Optimization results of both present and previous studies in the literature are also verified by finite element code.

Based on the studies carried out, we have concluded with the following results:

1. The natural frequncy increases with respect to increasing aspect ratios for the same number of layers. The designed plates having aspect ratio of 5 is more resistant than the others in terms of vibration.
2. It is observed that natural frequencies decrease with decreased constraint on the edges of plate. As the number of clamped in boundary condition of plate increases, first natural frequency values of composite plate increase considerably. Such as Ω = 11.920 for boundary condition SSFF whereas Ω = 93.694 for boundary condition CCCC. Since clamped boundary condition have less degree of freedom, it is more effective to stiffen the structure.
3. The results also showed that there is no a change in natural frequency when number of layers is increased, so the maximum natural frequency and the optimum fiber oriantations are not affected from increasing number of layers at constant thickness.
4. It is seen that, when rate in orthotropy degree of material is increased, maximum natural frequency values increase. Therefore, It is possible to increase the free vibration characteristics of the laminated composite plate by choosing the material having bigger rate of E_1/E_2.
5. The comparison study of conventional and continuous designs are performed to determine the effect of stacking sequence on vibration and the results showed that the optimal continuous designs are more stable than conventional designs.
6. Considering the hybrid algorithm against a single stochastic algorithm, the results of this study show that the hybrid optimization algorithm can be efficiently applied to find optimal stacking sequences of laminated composite plate and the hybrid algorithm converges faster than genetic algorithm.
7. Mode shapes corresponding to first natural frequency are obtained in the modal analysis. Even though the natural frequency parameters of composite plates increase in increasing aspect ratio, the corresponding mode shapes are similar to each other. It can be said that modes are inherent properties of a structure and they do not depend on aspect ratio of the plate and loads acting on the structure. Modes change if the material properties (mass, stiffness, damping properties), or boundary conditions (mountings) of the structure change.

REFERENCES

Abachizadeh, M., Tahani, M., 2008, An ant colony optimization approach to multi-objective optimal design of symmetric hybrid laminates for maximum fundamental frequency and minimum cost. *Struct Multidisc Optim* 37:367–376.

Adali, S., Verijenko, V. E., 2001, Optimum stacking sequence design of symmetric hybrid laminates undergoing free vibrations, *Composite Structures* 54 131–138.

Akovali, G., 2001, *Handbook of Composite Fabrication*, Smithers Rapra Technology.

ANSYS 10.0 Reference Manual, ANSYS Inc.

Apalak, M. K., Yildirim, M., Ekici, R., 2008, Layer optimisation for maximum fundamental frequency of laminated composite plates for different edge conditions. *Composite Science and Technology*, 68(2):537–50.

Ashby, M. F., 1987, Technology of the 1990s: Advanced Materials and Predictive Design, *Philosophical Transactions of the Royal Society of London*, A322, 393-407.

Aydin, L., Artem, H. S., 2011, Comparison of stochastic search optimization algorithms for the laminated composites under mechanical and hygrothermal loadings. *J Reinf Plast Compos*;30(14):1197–212.

Bert, C. W., 1977, Optimal design of a composite-material plate to maximize its fundamental frequency, *Journal of Sound and Vibration* 50(2): 229–37.

Bert, C. W., 1978, Design of clamped composite-material plates to maximize fundamental frequency, *Journal of Mechanical Design* 100(2): 274.

Blevins, R. D., 1979, *Formulas for Natural Frequency and Mode Shape*, New York: Van Nostrand Reinhold.

Campbell, F. C., 2010, *Introduction to Composite Materials*, Materials Park, OH: ASM International.

Daniel, Isaac M. and Ishai, Ori, 1994, *Engineering Mechanics of Composite Materials*, Oxford University Press.

Deveci, H. A., Artem, H. S., 2017, Optimum design of fatigue-resistant composite laminates using hybrid algorithm. *J Reinf Plast Compos*;168:178–188.

Duffy, K. J., Adali, S., 1991, Optimal fiber orientation of antisymmetric hybrid laminates for maximum fundamental frequency and frequency separation, *Journal of Sound and Vibration* 146 181–190.

Elmarakbi, A., 2014, *Advanced Composite Materials for Automotive Applications*: *Structural Integrity and Crashworthiness*, Wiley, ISBN 978-1-118-42386-8

Fan, S. C., Cheung, Y. K., 1984, Flexural free vibration of rectangular plates with complex support conditions, *J of Sound and Vib*, 93(1), 81-94.

Fang, C., Springer, G. S., 1993, Design of composite laminates by a Monte Carlo method. *J Compos Mater*; 27(7):721–53.

Gibson, R. F., 1994, *Principles of Composite Material Mechanics*, McGraw-Hill Book Co.

Grenestedt, J. L., 1989, Layup optimization and sensitivity analysis of the fundamental eigen frequency of composite plates. *Compos Struct* 12:193–209

Gurdal, Z., Haftka, R. T. and Hajela, P., 1999, *Design and optimization of laminated composite material*, John Wiley & Sons, Inc.

Hemmatian, H., Fereidoon, A., Sadollah, A., 2013, Optimization of laminate stacking sequence for minimizing weight and cost using elitist ant system optimization. *Advances in Engineering Software* 57: 8-18.

Karakaya, Ş., Soykasap, Ö., 2011, Natural frequency and buckling optimization of laminated hybrid composite plates using genetic algorithm and simulated annealing. *Struct Multidiscip Optim* 43, 61–72.

Kayikci, R., Sonmez, F. O., 2012, Design of composite laminates for optimum frequency response, *Journal of Sound and Vibration*, 331:1759-1776.

Kaw, Autar K., 2006, *Mechanics of Composite Materials*, Taylor & Francis Group, LLC.

Kollar, L. P., Springer, G., 2003, *Mechanics of Composite Structures*, Cambridge University Press, 480, New York.

Logan, D. L., 2011, *A first Course in the Finite Element Method*, 2nd ed., PWS-Kent Publishers, Boston, MA.

Lopez, R. H., Luersen, M. A. and Cursi, E. S., 2009, Optimization of laminated omposites considering different failure criteria. *Composites Part B: Engineering*. 40(8): p. 731-740.

Mallick, P. K., 2007, *Fiber-reinforced Composites: Materials, Manufacturing, and Design*, Taylor & Francis Group, LLC.

Mateus, H. C., Soares, C. M. M., Soares, C. A. M., 1991, Sensitivity analysis and optimal design of thin laminated composite structures, *Computers & Structures* 41(3): 501–508.

Mazumdar, S. K., 2002, *Composite Manufacturing: Materials, Product and Process Engineering*, CRC Press, LLC

Narita, Y., 2003, Layerwise optimization for the maximum fundamental frequency of laminated composite plates, *Journal of Sound and Vibration* 263 1005–1016.

Nicosia, G., & Stracquadanio, G. ,2008, Generalized pattern search algorithm for peptide structure prediction. *Biophysical Journal*, 95(10), 4988-4999.

Optimization ToolboxTM, MATLAB computer software in version R2016a, *The Mathworks Inc*; 2016.

Rao, Singiresu S., 2009, *Engineering Optimization: Theory and Practice*, John Wiley & Sons, Inc.

Reddy, J. N., 2004, *Mechanics of Laminated Composite Plates and Shells*, CRC Press.

Reiss, R., Ramachandran, S., 1987, Maximum frequency design of symmetric angle-ply laminates, *Composite Structures* 4, Vol. 1: *Analysis and Design Studies*, *Elsevier, London,* pp. 1476–1487.

Sadr, M. H., Ghashochi Bargh, H., 2011, Optimization of laminated composite plates for maximum fundamental frequency using Elitist-Genetic algorithm and finite strip method. *Journal of Global Optimization* 54, no. 4: 707-28.

Qatu, M. S., 1991, Free vibration of laminated composite rectangular plates. *Int. J. Solids Struct*. 28(8), 941–954.

Xin-SheYang, 2010, *Engineering Optimization: an Introduction with Metaheuristic Applications*, John Wiley & Sons, Inc.

APPENDIX A

MATLAB COMPUTER PROGRAM

```
function f=naturalfrequency(x)

E1 = 138*10^9; %[Pa]
E2 = 8.96*10^9; %[Pa]
G12 = 7.1*10^9;
v12 = 0.3;
v21=v12*(E2/E1);
ro =3.2;
b = 0.20;
r = 2; % plate aspect ratio
a = b/r;
n = 8; % number of plate
tp = 0.002; %thickness of plate
Q11=E1/(1-v12*v21);
Q12=(v21*E1)/(1-v12*v21);
Q22=E2/(1-v12*v21);
Q66=G12;


m=n+1;
for j=1:m
   z(j)=-(tp/2-((j-1)*(tp/n)));
end
x_half = [x(1) x(2) x(3) x(4)];
x=[x_half fliplr(x_half)]; %mirror komutudur fliplr
D=zeros(3,3);
for k=1:n
c=cos(x(k)*pi/180);
s=sin(x(k)*pi/180);


Qbar11=Q11*c^4+2*(Q12+2*Q66)*s^2*c^2+Q22*s^4;
Qbar12=(Q11+Q22-4*Q66)*s^2*c^2+Q12*(s^4+c^4);
Qbar22=Q11*s^4+2*(Q12+2*Q66)*s^2*c^2+Q22*c^4;
Qbar16=(Q11-Q12-2*Q66)*s*c^3+(Q12-Q22+2*Q66)*s^3*c;
Qbar26=(Q11-Q12-2*Q66)*s^3*c+(Q12-Q22+2*Q66)*s*c^3;
Qbar66=(Q11+Q22-2*Q12-2*Q66)*s^2*c^2+Q66*(s^4+c^4);

Qbar=[Qbar11 Qbar12 Qbar16;Qbar12 Qbar22 Qbar26;Qbar16 Qbar26 Qbar66];
D(1,1)=D(1,1)+Qbar11*(z(k+1)^3-z(k)^3)/3;
D(1,2)=D(1,2)+Qbar12*(z(k+1)^3-z(k)^3)/3;
D(1,3)=D(1,3)+Qbar16*(z(k+1)^3-z(k)^3)/3;
D(2,2)=D(2,2)+Qbar22*(z(k+1)^3-z(k)^3)/3;
D(3,3)=D(3,3)+Qbar66*(z(k+1)^3-z(k)^3)/3;
D(2,3)=D(2,3)+Qbar26*(z(k+1)^3-z(k)^3)/3;
```

```
end
D(2,1)=D(1,2);
D(3,2)=D(2,3);
D(3,1)=D(1,3);
D=[D(1,1) D(1,2) D(1,3);D(2,1) D(2,2) D(2,3);D(3,1) D(3,2) D(3,3)];


G1= 1.25;

G2= 0.597;

H1= 1.165;

H2= -0.0870;

J1= 1.165;

J2= 0.471;

omega=((pi^2/(4*ro))*((D(1,1)*((G1/b)^4))+(D(2,2)*(G2/a)^4)+((2*H1*H2*(D(1,2)+(2*D(3,3
))))/((a^2)*(b^2)))+((4*D(3,3)*(J1*J2-H1*H2))/((a^2)*(b^2)))))^0.5;

R=(E2*(tp^3))/(12*(1-v12*v21));

gama=omega*pi*2*(b^2)*((ro/R)^0.5);

f=-min(gama);
```

APPENDIX B

ANSYS APDL CODE

```
/PREP7                          ! Preprocessor module
!*
ET,1,SHELL281                   ! Choose SHELL281 element for analysis
!*
KEYOPT,1,1,0
KEYOPT,1,8,1
KEYOPT,1,9,0

MPTEMP,,,,,,,,                  ! Material properties
MPTEMP,1,0
MPDATA,EX,1,,138E9
MPDATA,EY,1,,8.96E9
MPDATA,EZ,1,,8.96E9
MPDATA,PRXY,1,,0.3
MPDATA,PRYZ,1,,0.3
MPDATA,PRXZ,1,,0.3
MPDATA,GXY,1,,7.1E9
MPDATA,GYZ,1,,7.1E9
MPDATA,GXZ,1,,7.1E9
MPTEMP,,,,,,,,
MPTEMP,1,0
MPDATA,DENS,1,,1600

sect,1,shell,,                  ! Section shell set
secdata, 0.00025,1,0,3          ! 1st layer: mat. , 0 deg, t=0.00025m
secdata, 0.00025,1,90,3         ! 2nd layer: mat. , 90 deg, t=0.00025m
secdata, 0.00025,1,0,3          ! 3rt layer: mat. , 0 deg, t=0.00025m
secdata, 0.00025,1,90,3         ! 4th layer: mat. , 90 deg, t=0.00025m
secdata, 0.00025,1,90,3         ! Same layers in symmetrical order
secdata, 0.00025,1,0,3
secdata, 0.00025,1,90,3
secdata, 0.00025,1,0,3
secoffset,MID                   ! Nodes on the laminate middle thickness
seccontrol,,,, , , ,
K,1,0.2,0,,                     ! Creates a rectangle
K,2,0,0.2,,
K,3,0,0,,
K,4,0.2,0.2,,
K,4,0.2,0.2,,

LSTR,     3,     1
LSTR,     1,     4
LSTR,     4,     2
```

```
LSTR,      2,      3
FLST,2,4,4
FITEM,2,1
FITEM,2,2
FITEM,2,3
FITEM,2,4
AL,P51X

ESIZE,0,50,                          ! No. of element divisions = 50
MSHAPE,0,2D
MSHKEY,0
CM,_Y,AREA
ASEL, , , ,      1
CM,_Y1,AREA
CHKMSH,'AREA'
CMSEL,S,_Y

AMESH,_Y1

FLST,2,1,4,ORDE,1                    ! Impose clamped boundary condition
FITEM,2,4
DL,P51X, ,ALL,0
FLST,2,1,4,ORDE,1
FITEM,2,1

DL,P51X, ,ALL,0
FLST,2,1,4,ORDE,1
FITEM,2,2

DL,P51X, ,ALL,0
FLST,2,1,4,ORDE,1
FITEM,2,3

DL,P51X, ,ALL,0
FINISH
/SOL
ANTYPE,2                             ! Modal analysis option

MODOPT,LANB,7
EQSLV,SPAR
MXPAND,7, , ,0
LUMPM,0
PSTRES,0
MODOPT,LANB,7,0,1000000000, ,OFF
/STATUS,SOLU
SOLVE
FINISH                               ! Exit solution module
/POST1                               ! Post-processor module
SET,LIST                             ! List solutions
```